frontiers in Earth Science

ORIGINAL RESEARCH
published: 29 May 2020
doi: 10.3389/feart.2020.00160

The Tail of the Late Jurassic Sauropod *Giraffatitan brancai*: Digital Reconstruction of Its Epaxial and Hypaxial Musculature, and Implications for Tail Biomechanics

Verónica Díez Díaz[1,2], Oliver E. Demuth[3,4], Daniela Schwarz[1] and Heinrich Mallison[5,6]*

[1] Museum für Naturkunde Leibniz-Institut für Evolutions- und Biodiversitätsforschung, Berlin, Germany, [2] Humboldt Universität zu Berlin, Berlin, Germany, [3] Structure and Motion Laboratory, Royal Veterinary College, Hatfield, United Kingdom, [4] School of Earth Sciences, University of Bristol, Bristol, United Kingdom, [5] Center of Natural History (CeNak), University of Hamburg, Hamburg, Germany, [6] Palaeo3D, Pöttmes, Germany

OPEN ACCESS

Edited by:
Pasquale Raia, University of Naples Federico II, Italy

Reviewed by:
Peter Lewis Falkingham, Liverpool John Moores University, United Kingdom
Ryan T. Tucker, Stellenbosch University, South Africa

***Correspondence:**
Verónica Díez Díaz
diezdiaz.veronica@gmail.com

Specialty section:
This article was submitted to Paleontology, a section of the journal Frontiers in Earth Science

Received: *31 January 2020*
Accepted: *29 April 2020*
Published: *29 May 2020*

Citation:
Díez Díaz V, Demuth OE, Schwarz D and Mallison H (2020) The Tail of the Late Jurassic Sauropod Giraffatitan brancai: Digital Reconstruction of Its Epaxial and Hypaxial Musculature, and Implications for Tail Biomechanics. Front. Earth Sci. 8:160. doi: 10.3389/feart.2020.00160

Dinosaur locomotion and biomechanics, especially of their pelvic girdles and hindlimbs, have been analyzed in numerous studies. However, detailed volumetric musculoskeletal models of their tails are rarely developed. Here, we present the first detailed three-dimensional volumetric reconstruction of the caudal epaxial and hypaxial musculature of the Late Jurassic sauropod *Giraffatitan brancai*, and highlight the importance and necessity of 3D modeling in musculoskeletal reconstructions. The tail of this basal macronarian is relatively short compared to diplodocids and other coexisting macronarians. The center of mass lies well in front of the hindlimbs, which support only ca. half the body weight. Still, our reconstruction suggests a total weight for the entire tail of ca. 2500 kg. We conclude that the hypaxial and tail-related hindlimb muscles (most specifically the *M. caudofemoralis longus* and its counterpart the *M. ilioischiocaudalis*) in *Giraffatitan* were well developed and robustly built, compensating for the shorter length of the *M. caufodemoralis longus*, the main hindlimb retractor muscle, in comparison with other sauropods. Our methodology allows a better-constrained reconstruction of muscle volumes and masses in extinct taxa, and thus force and weight distributions throughout the tail, than non-volumetric approaches.

Keywords: sauropoda, Tendaguru, *Giraffatitan*, volumetric musculoskeletal modeling, tail

INTRODUCTION

Reconstructions of the musculoskeletal system of dinosaurs have been inferred from the anatomical comparison of and the inference of homological structures in closely related or osteologically similar animals (e.g., Dilkes, 1999; Carrano and Hutchinson, 2002) based on the extant phylogenetic bracket (EPB) (Bryant and Russell, 1992; Witmer, 1995, 1997). Key examples for this are the highly esteemed and classical publications of Romer (e.g., Romer, 1923), which rely on thorough studies of the anatomy of living taxa. In the case of dinosaurs, numerous publications (e.g., Dilkes, 1999; Carrano and Hutchinson, 2002; Hutchinson, 2002; Organ, 2006; Schwarz-Wings, 2009; Allen, 2010) have analyzed the muscles of the limbs and the axial skeleton of living archosaurs (i.e., crocodilians

and birds), and extrapolated this information to infer it on to the preserved osteological remains of extinct taxa.

Musculature and ligaments often leave characteristic traces (= osteological correlates, Witmer, 1995) on the bone surface of all vertebrates. Where such osteological correlates for muscles are present on the vertebrae in both sauropods and crocodilians, these muscles can be reconstructed as level II inference (Witmer, 1995, 1997). However, variation in the soft tissue configuration and uncertainties in the interpretation of osteological correlates demand a cautious approach in reconstructing soft tissue anatomy of extinct taxa (Bryant and Russell, 1992; Witmer, 1995; Carrano and Hutchinson, 2002). Sauropod vertebrae expose a complex surface pattern of laminae, fossa, ridges, bulges and rugosities, which are associated with pneumatic structures and attachment sites of muscles, tendons and ligaments (Wedel et al., 2000; Wedel, 2003a,b, 2009; O'Connor, 2006; Schwarz-Wings, 2009). Unambiguous pneumatic structures can be distinguished from correlates for muscles and ligaments by the presence of pneumatic foramina that penetrate deeply into the bone (O'Connor, 2006).

Over the last few years, vertebrate paleontology took advantage of novel techniques and software (Cunningham et al., 2014; Sutton et al., 2014). Digitization methodologies (e.g., CT scanning and photogrammetry, see Mallison and Wings, 2014; Fahlke and Autenrieth, 2016) and Computer-Aided-Design (CAD) tools made it possible to capture the morphology of the bones upon which three-dimensional reconstructions of the musculoskeletal system of extinct animals could be improved. The spatial organization of muscle groups can be assessed in 3D and thus intersections of individual muscles prevented. These three-dimensional reconstruction methods have overwhelmingly focused on cranial and especially adductor musculature (Lautenschlager, 2013; Sharp, 2014; Button et al., 2016; Gignacand Erickson, 2017), while the axial musculature received little attention. The myological reconstruction of the dinosaur tail in particular is a complex task, as it consists of ten individual muscles, partly subdivided into multiple heads. Previous studies on dinosaur tail musculature have primarily focused on the *M. caudofemoralis longus* (CFL) (e.g., Mallison, 2011; Persons and Currie, 2011, 2012; Persons et al., 2014), because of its locomotive importance as the main hindlimb retractor muscle. However, none has attempted to reconstruct the complete musculoskeletal system of the tail. Here we present the reconstructed caudal anatomy of *Giraffatitan brancai* based on the comparison of the caudal vertebral anatomy, which has previously been described in great detail (e.g., Janensch, 1914, 1950a, 1961; Paul, 1988; Taylor, 2009), and muscle attachments with those of extant crocodilians.

The axial skeleton of *Giraffatitan* has been described extensively (Janensch, 1950a), and a reconstruction was also suggested for the mounted skeleton (Janensch, 1950b). Modern anatomical knowledge was later used to establish a new mount of the skeleton, on display at the Museum für Naturkunde Berlin (MfN) since 2007 (Remes et al., 2011). In the first mount and descriptions, Janensch (1950b) suggested an anteriorly ascending posed dorsal column, induced by the long forelimbs and high anterior trunk, and accordingly a matching tilted position of the sacrum. The lack of keystoning in the anterior caudal vertebrae convinced Janensch (1950b) that the anterior tail of *Giraffatitan* extended from the hips in a straight, thus caudally descending line, in contrast to the tails of other sauropods, which emerged from the hips horizontally. This posture led to the tail contacting the ground much further anteriorly in relation to its overall length than in the other species Janensch (1950b) mentioned: *Dicraeosaurus hansemanni*, *Diplodocus carnegii* and *Camarasaurus lentus*. During a general renovation of the Berlin dinosaur exhibition hall (between 2005 and 2007), the mounted skeleton was rebuilt. The new mount differs from the old mount in several key characteristics (Remes et al., 2011):

- Improvements to the models of the presacral vertebrae and head,
- The posture of the neck, the shape of the torso,
- The orientation of the pectoral girdle and forelimbs, and
- The posture of the tail, still emerging from the hip caudally descending, but curving slightly dorsally to remain well clear of the ground.

Here, we digitally reconstruct the tail of this sauropod. We applied photogrammetric 3D digitization and 3D modeling tools in combination with information provided by dissections of extant crocodilians (*Alligator mississippiensis*) (**Supplementary Figure S1**) and an Extant Phylogenetic Bracket (EPB; Witmer, 1995) approach by comparing the anatomy of the caudal vertebrae and muscles of *Giraffatitan* with that of extant crocodilians. The other side of the bracket, birds, shows a strongly reduced caudal musculoskeletal system, which is adapted for novel functions in flight and display (e.g., Gatesy and Dial, 1996; O'Connor et al., 2013). Bird tails are much shorter, with fewer vertebrae, of which up to half are co-ossified into the pygostyle. Just anterior to the pygostyle, there is a maximum of six mobile vertebrae present, depending on the species (Gatesy and Dial, 1996). Furthermore, changes between the thoracic and caudal epaxial musculature are hypothesized to coincide with the evolution of the synsacrum (a structure highly involved in the flight, together with the notarium, see Organ, 2006). For example, caudal epaxial muscles were decoupled from their locomotor function on the evolutionary line to birds (Gatesy and Dial, 1996), and several muscles were lost (e.g., *Mm. interspinales* and *M. multifidus*). In addition, due to the absence of chevrons, the attachments of the tail depressor muscles shifted to the transverse processes, among further modifications (Pittman et al., 2013). The absence of chevrons and the truncation of the bird tail also relate to a reduction of the hypaxial *M. caudofemoralis* in birds, but also in maniraptoran theropods, as hypothesized from the lack of a clearly distinguishable fourth trochanter (Gatesy, 1991a; Rashid et al., 2014). In addition, the origin of the *M. caudofemoralis longus* in birds, where present, is on the pygostyle (e.g., Gatesy, 1991a). These changes on the skeleton and muscle modifications, especially the ones related to the hypaxial musculature, led to a decoupling of the locomotor structures from each other (Gatesy and Dial, 1996; Dececchi and Larsson, 2013), therefore in extant birds the reduced tail muscles have lost their propulsion function and connection

to the hindlimbs. This leaves only extant crocodilians as a model for the configuration and architecture of the caudal musculature for sauropod dinosaurs. Modern crocodilians can be used to infer the set of epaxial and hypaxial tail muscles present in sauropod dinosaurs, especially given the similarities in the osteological correlates (see below). The musculoskeletal system of the crocodilian tail has been described in detail by many researchers (e.g., Hair, 1868; Romer, 1923; Frey, 1982a,b, 1988; Frey et al., 1989; Cong et al., 1998; Hutchinson and Gatesy, 2000; Wilhite, 2003; Allen et al., 2014). We focused on these publications for the reconstruction of the tail muscular anatomy of *Giraffatitan brancai*. We follow the homologization of different epaxial and hypaxial muscle groups in archosaurs by Tsuihiji (2005, 2007).

In addition, crocodilians are the sole living large reptiles that can walk with the belly and most of the tail being held off the ground. They lift their tail from the ground during high walk (distal half of tail sometimes on the ground, proximal half lifted up) and gallop (tail lifted completely), although this is not employed over long distances (see e.g., Cott, 1961; Webb and Gans, 1972; Zug, 1974; Gatesy, 1991b; Hutchinson et al., 2019). This makes them the closest available analog to sauropod dinosaurs.

Institutional abbreviations: MB.R. Museum für Naturkunde Berlin, Berlin, Germany.

MATERIALS AND METHODS

Material

The lectotype of *Giraffatitan brancai* (Taylor, 2009, 2011) is the partial skeleton SI (MB.R.2180), and the paralectotype is SII (MB.R.2181). The mounted skeleton in the exhibition of the Museum für Naturkunde (**Figure 1**) is a composite reconstruction, consisting mostly of MB.R.2181 (SII), and including elements of MB.R.2180 (SI), duplicates of some bones, and plaster reconstructions of the missing parts (Janensch, 1950b; Remes et al., 2011). However, neither SI nor SII included caudal vertebrae, even though other skeletal remains of *Giraffatitan* were found in the same quarry "S" in the Tendaguru area. Therefore, Janensch used the vertebrae from quarry "no," MB.R.5000, for the mount (Janensch, 1950b).

In total, three caudal series are known from the Tendaguru area for *Giraffatitan brancai*: MB.R.5000 (from quarry "no"), MB.R.2921 (from quarry "Aa") and MB.R.3736 (from quarry "D").

Giraffatitan brancai had ca. 50–60 caudal vertebrae.

- The longest caudal series recovered has 50 caudal vertebrae (MB.R.5000). It consists of the second to fifty-first caudal vertebrae (Janensch, 1950a). As Janensch (1950a) states, these caudal vertebrae were found "not articulated, with the exception of a few at the end, but altogether relatively in sequence."
- Series MB.R.3736 consists of 29 caudal vertebrae. The first 23 caudal vertebrae (from the second to the twenty-fourth of the series) were found in articulation, and the rest (from the twenty-sixth to the thirty-second, missing the thirty-first) were found associated (Janensch, 1950a). No chevrons were found next to this caudal series.
- Series MB.R.2921 consists of the first 18 caudal vertebrae (MB.R.2921.1-18) and fourteen of their chevrons (MB.R.2921.19-32), found in an articulated sequence behind the last sacral vertebra (Janensch, 1950a).

Janensch (1950a,b) mentioned severe taphonomic damage to series "no" (MB.R.5000), including shrinking of many centra. Additionally, there are some anatomical differences between MB.R.5000 and the other two caudal series, in particular concerning the presence of pneumatic features (Wedel and Taylor, 2013). Series MB.R.5000 was therefore used only for comparative purposes for this study, especially considering that access to it on the mount is difficult. Series MB.R.2921 and MB.R.3736 resemble each other in osteology, and were therefore primarily used for this study. For the analysis of the anatomical features both these caudal series were studied, but only MB.R.2921 (the better preserved series) was used for the three-dimensional reconstruction of the musculoskeletal system. Especially information on the neural arches and the epaxial musculature could be more confidently obtained in the caudal series MB.R.2921 and its elements are overall more complete than those of MB.R.3736.

Series MB.R.2921 shows some obvious damage: the left transverse processes of caudal vertebrae 1–3, 5–7, and 9 are missing, as is the right transverse processes of caudal vertebra 4, while those of caudal vertebrae 3 and 5 are damaged. The left prezygapophyses of all vertebrae within the entire series are well preserved, but the right prezygapophysis is missing in caudal vertebra 3. The postzygapophyses are all preserved but for the right one in caudal vertebra 2.

The damage in series MB.R.3736 is far more extensive. Only a small number of caudal vertebrae preserve zygapophyses, and most neural arches and spines as well as transverse processes are missing or badly damaged. The centra, in contrast, are mostly well preserved.

One partial sacrum was found in the same quarry "Aa," as were the caudal series MB.R.2921 (Janensch, 1950a, fig. 74). However, this sacrum could not be re-located in the collections of the MfN, and it must be assumed that the original fossil was lost during WWII. A simplified cast of it exists in the skeletal mount. For the development of the three-dimensional musculoskeletal model we used this sacrum cast MB.R.5003, as well as the right femur MB.R.5016 (quarry number "Ni"), right tibia MB.R.2181.84 (quarry number "SII") and right fibula MB.R.2181.85 (quarry number "SII") on display, adjusting their size to match the caudal series.

Methods

The fossils were digitized via photogrammetry, following the protocols of Mallison and Wings (2014), and the updated version of Mallison et al. (2017). A digital SLR camera (Canon EOS 70D with Canon 10–18 mm f4.5-5.6 lens) was used with a LED ring light. Images were processed in Agisoft

FIGURE 1 | The current mount (on display since 2007) of the Late Jurassic sauropod *Giraffatitan brancai* (foreground) at the main hall of the Museum für Naturkunde (Berlin, Germany). Photograph by Antje Dittmann (MfN).

PhotoScan Professional v.1.4.0[1], in order to obtain three-dimensional models of each bone. High-quality polygon mesh files were created (approximately 5 million polygons and 250 MB as binary STL files each) for curatorial and museological purposes, but also lower resolution color-free STL files (50.000 polygons) for the musculoskeletal modeling and biomechanical analysis presented here.

Several chevrons were poorly preserved, some with missing parts, e.g., the distal part of the blade, or one of the rami (MB.R.2921.19-20, 24, 29-30, 31). These elements were digitally restored in zBrush 4R7 (Pixologic)[2], either by mirroring the preserved ramus, or by scaling and superimposing the distal part of the blade of adjacent chevrons. The two missing chevrons, 1 and 12, were entirely created digitally. Chevrons MB.R.2921.19 (the second) and MB.R.2921.29 (the thirteenth) were used as proxy models and scaled to fit into the sequence, but also to the articular facets of their corresponding caudal vertebrae.

All 3D models were imported into Rhinoceros 5.0 (McNeel Associates)[3] and articulated in the osteological neutral pose (ONP, after Stevens and Parrish, 1999, 2005a,b; Mallison, 2010a,b) following the protocol described by Mallison (2010a,b): individual vertebrae were articulated in pairs to minimize the impact of preconceived ideas (e.g., overall downward position of the tail, as in the former reconstruction of the mounted skeleton of *Giraffatitan*). Additionally five cartilaginous neutral poses (CNP, after Taylor, 2014) were assessed to test the influence of the intervertebral cartilage on the muscle volume.

As previously commented, we only can rely for a 50% EPB level I inference when reconstructing most of the muscles in terms of insertions and passages, as we only have one part of the bracket (i.e., crocodilians). However, the general presence of the reconstructed muscles for tail and femur are present also in birds in most cases (e.g., the suite of epaxial muscles – at least until the pygostyle –, and the *M. caudofemoralis longus*), so a level II inference would only apply to the *M. ilioischiocaudalis*. Besides, and as already mentioned, those bones present in birds too (i.e., femur, sacrum and first two caudal vertebrae) are very strongly modified in extant taxa, as are the muscles because of their locomotionary differences. Morphologically, the sacrum and femur of sauropods are more similar to crocodilians than to birds, helping to confirm this level II inference.

The three-dimensional models of the musculature were created in the software package Autodesk Maya[4]. We used a polygon-based modeling approach, similar to the box modeling approach by Rahman and Lautenschlager (2017), to build each muscle individually from the origin to the insertion, on the

[1]http://www.agisoft.com

[2]http://pixologic.com/features

[3]www.rhino3d.com

[4]https://www.autodesk.com/products/maya/overview

basis of osteological correlates identified by study of the physical and digital specimen. This allowed us greater control over the flow of the muscle shape than in a NURBS-based approach (e.g., Persons and Currie, 2011; Persons et al., 2014). Finely segmented muscles, e.g., the transversospinalis group, were simplified into a single body.

Bone volumes were calculated with Rhinoceros 5.0, and muscle volumes with Maya. For the muscle mass we use the density value proposed by Méndez and Keys (1960) for mammalian muscles ($d = 1.06 \times 10^3$ kg/m^3), which is similar to the measurements obtained by Hutchinson et al. (2015) for the hindlimb muscles of an ostrich (*Struthio camelus*).

For the calculation of bone mass the following factors were taken into consideration. Most caudal vertebrae of *Giraffatitan* have small pneumatic fossa indicating a small amount of pneumatisation. Overall, the pattern of pneumatisation in *Giraffatitan* caudal vertebrae is variable and irregular (Wedel and Taylor, 2013). As the caudal vertebral centra have a high volume to surface ratio, we estimate their cortical portion to be rather smaller than in girdle bones, ribs, or complexly shaped presacral vertebrae, and the trabecular and marrow portion to be accordingly larger. The volumetric bone density is typically close to 2×10^3 kg/m^3 for long bones (e.g., Mohiuddin, 2013; Fletcher et al., 2018) and somewhat lower for marrow-rich bones, due to the lower density of marrow of ca. 1×10^3 kg/m^3. We here chose 1.5×10^3 kg/m^3 for overall bone volumetric density, expecting the amount of pneumaticity to be the main driver von average density variation in the tail of *Giraffatitan*.

RESULTS

Osteologically Neutral Pose (ONP)

For exact alignment we found the reduced size files with 50.000 polygons insufficiently detailed. We therefore worked with the higher-resolution files with five million polygons.

Initially, we used the prezygapophyses and postzygapophyses as proxy for assessing the correct articulation between vertebrae, assuming that given full zygapophyseal overlap and – as far as possible – sub-parallel centra faces, the distance between vertebral bodies probably reflects the approximate intervertebral cartilage volume (Christian and Preuschoft, 1996; Christian and Dzemski, 2007).

Articulating the zygapophyses of series MB.R.2129 with full overlap (**Figure 2E**) resulted in a nearly straight line of vertebrae, but tilted some of the centra around their vertical and longitudinal axes (**Figures 2A,B**). Also, a slight but noticeable asymmetry and "twisting" around various axes of most neural arches, including the postzygapophyses, induced a slight sigmoidal curve, initially to the left, then to the right. The deformations also caused a long-axis rotation in parts of the series, tilting the neural spines of caudal vertebrae 3 through 8 noticeably to the left (**Figure 2B**). Additionally, due to slight taphonomic deformation of some zygapophyses, we could not completely avoid small intersections between zygapophyses (e.g., between caudal vertebrae 17 and 18) or larger, unrealistic gaps in the zygapophyseal joints.

We therefore reassembled the series MB.R.2129 based on centra faces to create a more life-like, less taphonomy-influenced reconstruction (**Figure 2C**), with higher lateral symmetry, which we used for the 3D reconstruction of the musculature. This second articulation consequently suffers from some additional, massive intersection between zygapophyses. While the anterior rim of the first caudal vertebral centrum is markedly concave in lateral view, the posterior rim is flat in lateral view. In all other vertebrae, both the anterior and posterior rims of the centra are mostly flat in lateral view, allowing a straightforward assembly of the tail based on the centra faces. Therefore, we were able to create this centra-based articulation without any uncertainty with regards to the angles between the vertebrae.

The chevrons were positioned into the existing articulated caudal vertebral series by matching their anterior and posterior articular facets with the orientation of the ventral articulation surfaces of each centrum. A short space was retained between the chevron and the vertebra, representing the volume of the articular cartilage. We found that the centra faces could be retained in practically parallel orientation with the chevrons added.

Overall, series MB.R.2129 shows a slight curvature in lateral view, lifting the posterior end by ca. one full centrum height of caudal vertebra 18 compared to the trend of the first three vertebrae. Repeated "playing" with the bone trios (two vertebrae and their chevron) to optimize alignment tended to increase rather than decrease the curvature.

In the skeletal reconstruction of the MB.R.3736 series a slight sigmoidal shape is created by centra-only alignment in the long axis of the tail in lateral view, between the fifteenth and eighteenth vertebrae, and the terminal section bends slightly ventrally (**Figure 2D**).

Cartilaginous Neutral Poses (CNPs) (Figure 3)

Several previous studies analyzed the ONP of the neck of sauropods and the effect of the intervertebral cartilage (e.g., Taylor and Wedel, 2013a; Taylor, 2014; Vidal et al., 2020a and references therein), but there is scant published data on the effects of intervertebral cartilage within the tail. As stated by Taylor and Wedel (2013a) the thickness of the articular cartilage between the centra of adjacent vertebrae affects posture. In this work we also assess how this cartilage thickness affects the mass, volume, and extension of the musculature (see below). However, for extinct taxa we can only make assumptions about the cartilage that existed in life. For that, five CNPs (Taylor, 2014) with different cartilage thicknesses (2.5, 5, 10, 15, and 20%) were assessed. Cartilage thicknesses percentages were chosen after the calculations of Taylor and Wedel (2013a) and Taylor (2014) for the cervical vertebrae of several extant animals and sauropod taxa, as data on caudal series is no available yet. Cartilage thicknesses were calculated as percentages of the centrum lengths (**Supplementary Table S1**).

Intervertebral cartilage volumes were added to the previous ONP. Taylor (2014) quantified the angle of extension at intervertebral joints when different cartilage thicknesses were included. This extension occurs because the thin zygapophyseal

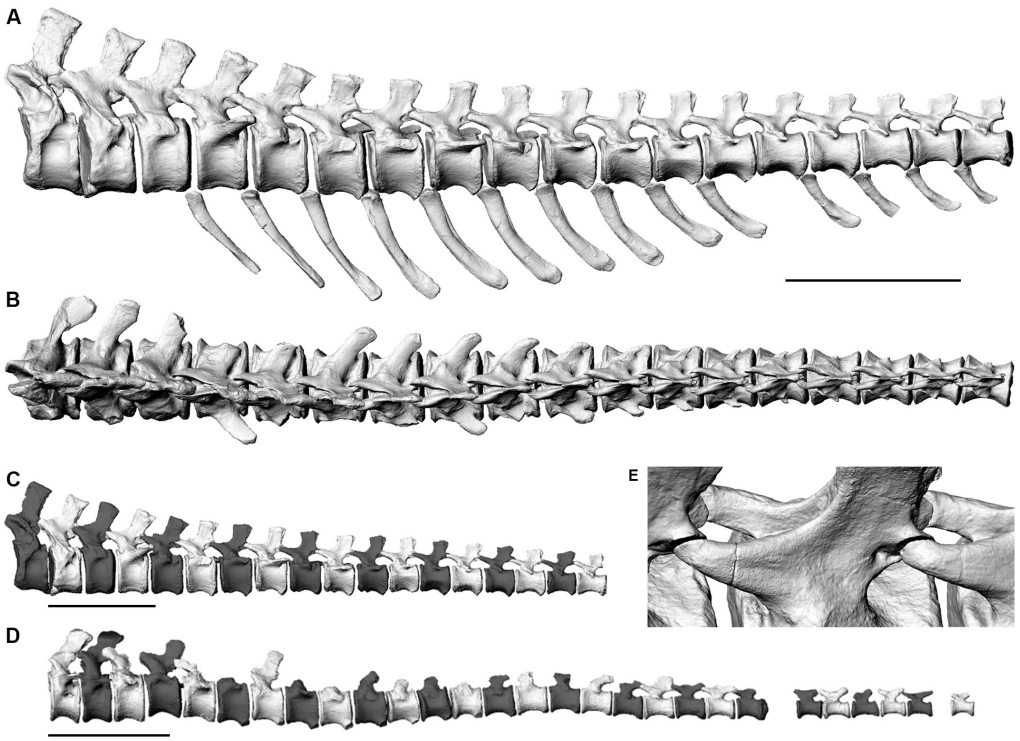

FIGURE 2 | Left lateral views **(A,C,D)** and dorsal view **(B)** of the three-dimensional skeletal reconstructions of two caudal vertebral series of the Late Jurassic sauropod *Giraffatitan brancai*. **(A–C)**. MB.R.2921 **(D)** MB.R.3736. **(A,B)** show alignment based on best fit of zygapophyses and sub-parallel centra, **(C,D)** show alignment based on centra faces. **(E)** Oblique close-up of the sets of zygapopyseal pairs (C 7–8 and C 8–9) from articulation in panels **(A,B)** aligned for best fit. Only the preserved remains have been illustrated here.

cartilage has no or negligible effect on the angle of extension between vertebrae, while the thick intervertebral one does: the angle of elevation at an intervertebral joint is increased when cartilage is included. This is true for opisthocoelous and procoelous vertebrae, but in the caudal series MB.R.2129 of *Giraffatitan* this dorsal or ventral extension is not present when different cartilage thicknesses are included, as these caudal vertebrae do not present condyles. Similar poses are obtained for the ONP and all the CNPs. However, it is important to state that in CNP 15% the zygapophyses start disarticulating from ca. seventeenth caudal onward, and in CNP 20% from the twelfth. An improved and more accurate model could be created by articulating the zygapophyses and thickening the base of the cartilage, resulting in a dorsal extension of the tail from this section. However, the cartilage volume is already thick at CNP 20%, and by increasing it in its base probably would lead to disarticulation of the chevrons too. Together with other results (see below) we do not consider this CNP 20% model as a possibility for a living animal. In the other CNPs the zygapophyses appear articulated, but a dorsal extension of the tail section that is not preserved could not be ruled out, as also seen in the CNP 15%. Besides, in the CNP 2.5 and 5% the caudal vertebrae are spaced very tightly, thus limiting movement of the tail, and furthermore making it impossible to correctly articulate the chevrons. Only the CNP 10% and 15% are therefore deemed possible for this caudal series.

Several sauropod caudal series have been found articulated or closely associated. Although it is uncertain linking the intervertebral spaces found in these articulated remains with the cartilage volume present in the living animal, we have checked them looking for hypothetical connections with our model. For example, the titanosaurian taxa *Oversosaurus* (Coria et al., 2013) and *Dreadgnothus* (Lacovara et al., 2014) preserved the first 20 caudal vertebrae articulated. Some measurements were made using the published material (figures, and a 3D model for the *Dreadgnothus* caudal series), and some interesting data were obtained: for *Overosaurus* intervertebral spaces of 26 to 28% the centrum length were calculated, while for *Dreadgnothus* the values changed along the series, being larger in the anterior section (ca. 40 to 44%) and decreasing through the series (20 to 22%). One specimen (DFMMh/FV 100) of the camarasauromorph *Europasaurus* presents an articulated caudal series of 13 vertebrae (Carballido and Sander, 2014). It was not possible to take accurate measurements as most of the vertebrae, although articulated, were displaced, but an intervertebral space of ca. 17–18% was calculated. The brachiosaurid *Padillasaurus* preserved the first eight caudal vertebrae in articulation (Carballido et al., 2015). The calculated intervertebral spaces were between 26 and 28%. However, this specimen presents a dorsal extension, so the calculated cartilage thicknesses are probably not comparable to the ones of the living animal. This dorsal extension of the tail is present in

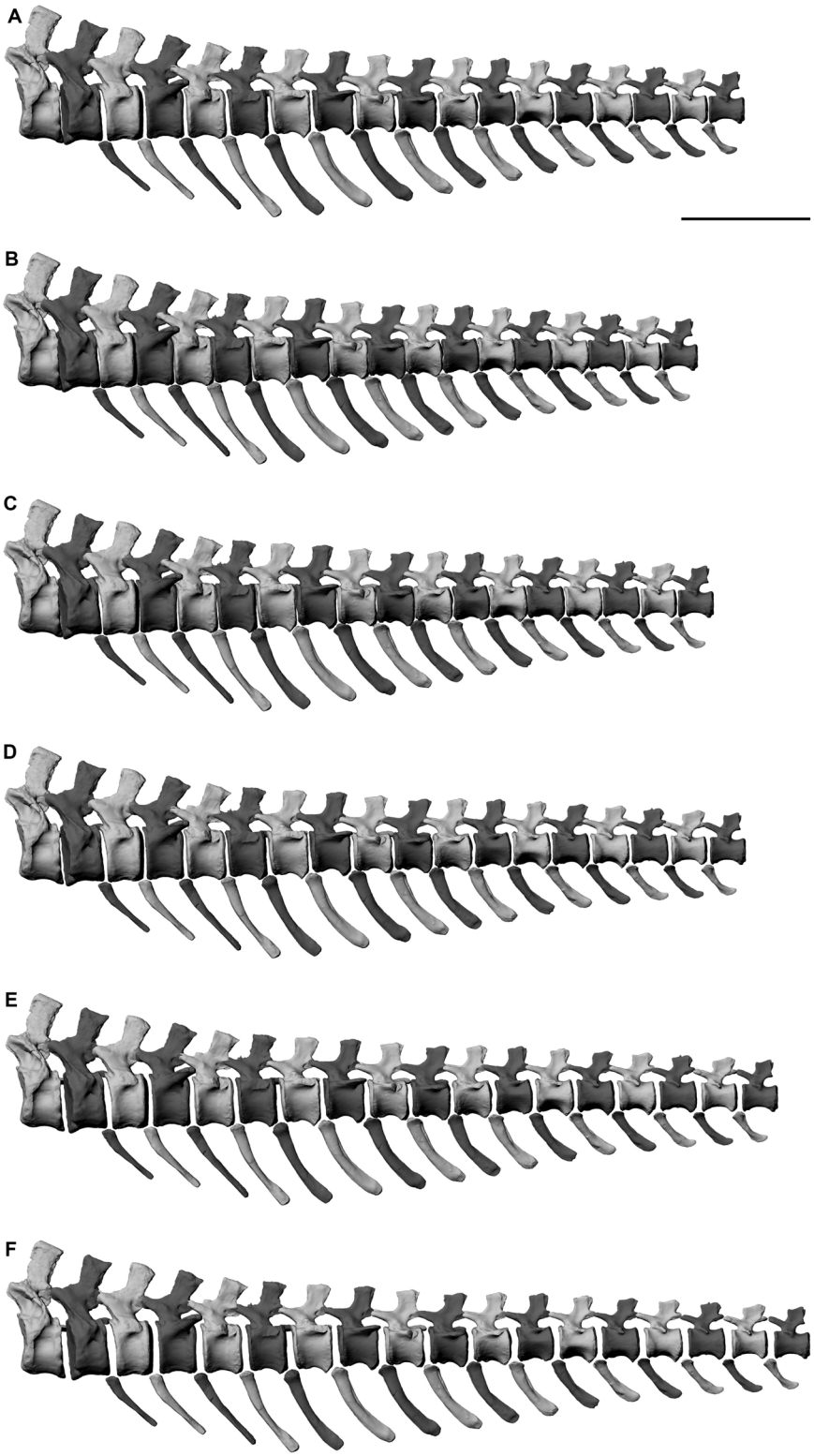

FIGURE 3 | Comparison between the **(A)** ONP, **(B)** CNP at 2.5%, **(C)** CNP at 5%, **(D)** CNP at 10%, **(E)** CNP at 15%, and **(F)** CNP at 20%. Scale = 50 cm.

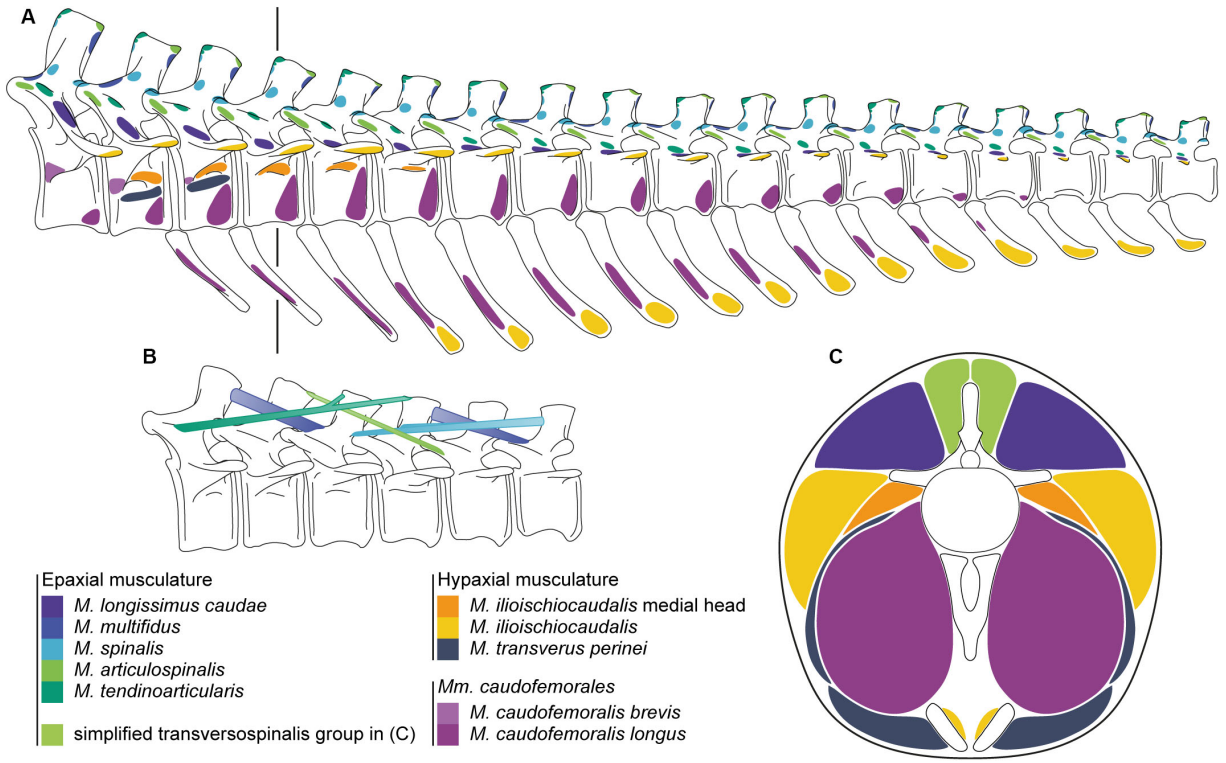

FIGURE 4 | (A) Origins and insertions of the caudal musculature of the Late Jurassic sauropod *Giraffatitan brancai*. **(B)** Simplified muscle paths of the transversospinalis group of the epaxial musculature. **(C)** Cross-section of the tail at the fourth caudal vertebrae showing the lateral extent of the tail musculature. The line in A indicates the location of the cross-section through the musculature. Paired ventral elements represent the ischia.

other sauropod caudal series, as *Camarasaurus* (Gilmore, 1925) or *Spinophorosaurus* (Remes et al., 2009). As already seen, numerous taphonomical factors need to be taken into account, so we cannot use these values with fidelity. Besides, they also indicate that cartilage thickness could highly vary through the caudal series, but also depend on the taxon. In addition, the articulation type between vertebrae (i.e., procoely, opisthocoely, etc.) probably affected this thickness too. A recent work on the caudal biomechanics of the titanosaur *Aeolosaurus maximus* suggests a cartilage thickness between 5 and 10% for the anterior section of the tail (Vidal et al., 2020b). More detailed work on these sauropod articulated caudal series needs to be undertaken to approach more accurately this issue.

Muscle Marks and Musculature Reconstruction

The caudal vertebrae and chevrons of *Giraffatitan* presents numerous osteological correlates related to the origins and insertions of the muscles and ligaments of the tail (**Figure 4** and **Supplementary Figure S1**). The inferred sets of epaxial and hypaxial muscles, together with the relevant hindlimb musculature for the correct reconstruction of the tail musculature (which are directly in or close to contact and/or restrict the volume of the tail musculature) are detailed in **Supplementary Table S2**.

Neural Arches

The lateral faces of the neural spines are slightly concave and show longitudinal (apicoventrally directed) rugosities, parallel to each other. At the apical edge of the neural spine both anterior and posterior processus – with different development stages depending on the position in the series – can be seen in form of the distal tips of both the prespinal and postspinal laminae. From caudal vertebra 3 on, the middle part of the tip of the neural spine is thickened, developing an apical prominence (slightly posteriorly displaced) from the fourth vertebra on. From caudal vertebra 8 on, this bulge shows sharp posterior edges in dorsoventral orientation on the lateral faces of the neural spines. In addition, three spurs are present in the neural spine laminae: two on the base of the spinoprezygapophyseal laminae, and one in the postspinal lamina. The spike present on the postspinal lamina appears in the caudal vertebrae 5, 6, 8–11, and 14. However, this feature could have been present in all caudal vertebrae with a distinct postspinal lamina. The prominences of the spinoprezygapophyseal laminae appear in the caudal vertebrae 2, 3, 5–7, although they were probably present from the first caudal vertebrae to the seventh. These osteological features correspond to the attachment of deep epaxial muscles (mediodistally) and *M. multifidus* (medially), and both the *M. spinalis* and *M. articulospinalis* (laterally). The *M. multifidus* originates from the distal posterior tip of the neural spine*M. articulospinalis* from the distal posterior tip.

Zygapophyses

The zygapophyses serve as attachment areas for the epaxial muscles including the *M. spinalis* (zygapophyseal joint capsule) and *M. articulospinalis* (lateral rugosity on the prezygapophyses). The *M. multifidus* inserts in a spur or rugosity on the spinoprezygaposeal lamina of the second next vertebra (from the first to the seventh vertebrae), or in the subtle dorsal rugosity on the prezygapophyses from the eighth vertebra onward. The *M. articulospinalis* inserts on a lateral rugosity of the prezygapophysis two vertebrae further down the tail. The development of the mentioned attachment structures also depend on the position in caudal series, being steadily reduced distally.

Vertebral Centra

Although the prezygodiapophyseal lamina is not well developed, an oblique bulge and rugosity can be seen between the prezygapophysis and the transverse process, which is interpreted as the osteological correlate for the insertion of the *M. tendinoarticularis*.

The transverse process is an important osteological correlate for both the epaxial and hypaxial muscles. Its distal tip is an insertion for the hypaxial musculature (dorsal aspect of the *M. ilioischiocaudalis*). A bulge and rugosity at the junction between the transverse process and the centrum (proximal tail) and longitudinal ridge (13th vertebra onward) acts as attachment for the bounding septum (Grenzseptum) between the lateral epaxial musculature (*M. tendinoarticularis* and *M. longissimus caudae*) and is further the insertion for the *M. longissimus caudae*. Transverse processes are present in all the caudal vertebrae of MB.R.2921, becoming smaller and rounder distally. In MB.R.3736 the transverse processes disappear by caudal vertebra 25 in the series. As they disappear, the mentioned longitudinal ridge persists close to the junction between the neural arch and the centrum, delineating the insertion of both the *M. longissimus caudae* (dorsally) and the *M. ilioischiocaudalis* (ventrally).

The major part of the *M. caudofemoralis brevis* originates from the medial surface of the postacetabular process of ilium and the ventral aspect of the last sacral rib. From there, the muscle extents distally and also attaches anterolaterally on the centra of caudal vertebrae 1 to 3.

The first two caudal centra of MB.R.2921 show a lateral concavity below the transverse processes, which we interpret as a space for cryptic diverticula (see below). However, between these depressions and the transverse process in caudal vertebra 2 there is a shallow shelf, there are subtle bumps on caudal vertebra 3 to 5 at this position, which we regard to be the attachment site of the medial head of the *M. ilioischiocaudalis* (see **Supplementary Figure S2**). Ventral to the lateral depression in caudal vertebra 2 and approximately at the same position on caudal vertebra 3 there is a faint ridge, which serves as the origin for the *M. transversus perinei*. The muscle extends laterally, wrapping around the *M. caudofemoralis longus* and the ischial ramus of the *M. ilioischiocaudalis* to insert on the distal lateral ischium and on the aponeurosis surrounding the cloaca.

The ventral half of the centrum is convex in the anteriormost nine vertebrae, and then becomes gradually more concave (just below the transverse process). In these anterior vertebrae the distal lateral surface of the centrum serves as attachment for the *M. caudofemoralis longus*. Caudal 11 (right side) and caudal 12 shows the first occurrence of a lateral broadening of the centrum at half its height, forming an incipient ridge, of which there is no trace in the previous vertebrae. This ridge gradually moves ventrally in the next three vertebrae on both sides, separating two lateral surfaces, and merging into the ventrolateral border of the centrum. We interpret this weakly developed ridge as the caudal limit of the *M. caudofemoralis longus*, constricting the muscle into a narrow tip well separated from the transverse processes, unlike the dorsally directed tapering seen in extant crocodiles. After the fourteenth caudal the ridge merges into the ventrolateral edge of the centrum; accordingly, the ventrolateral surface disappear entirely, indicating that the *M. caudofemoralis longus* does not extend distally beyond this point.

Chevrons

The lateral surfaces of the chevrons and their general morphology are important osteological correlates for the hypaxial musculature and their development. In the lateral surface of the chevrons, more dorsally located in the anterior ones, a weak oblique rugosity appears, for the insertion of the *M. caudofemoralis longus*. On the distal tip, in its lateral aspect, another rugosity, for the insertion of the ventral part of the *M. ilioischiocaudalis*, is apparent. The morphology of the distal blade of the chevrons changes along the series: the first three chevrons have a more acute distal blade, while the next ones have a more rounded and transversally compressed distal third. From the twelfth chevron (thirteenth caudal vertebra) onward, this distal third of the blade becomes more posteriorly directed. These differences in morphology reflect a change in the insertions and development of both *M. caudofemoralis longus* and *M. ilioischiocaudalis*.

Sizes, Masses and Volumes

From the addition of all individual bone and muscle masses (**Table 1** and **Supplementary Tables S3, S4**) we here suggest hypothetical weights for the preserved caudal series MB.R.2921, depending on the ONP and CNPs.

ONP

The caudal series MB.R.2921 presents a total length (from the first caudal vertebra to the last) of 280.82 cm when articulated in ONP. All the caudal bones (vertebrae and chevrons) weighted 106.92 kg (1775.67 kg with the pelvis and sacrum), and all the muscle (right and left) groups 950.07 kg. So the preserved caudal series MB.R.2921 of *Giraffatitan* approximately weighted 1056.99 kg in total (2725.74 kg with the pelvis and sacrum). The total volume of the caudal series is 967.57 liters (2080.07 liters with the pelvis and sacrum). It is important to keep in mind that not all the vertebrae were completely preserved (e.g., some of them were missing parts of the transverse processes), and some epaxial muscles have been simplified, but this should not affect the volume.

TABLE 1 | Comparison of the calculated volumes (l) and masses (kg) for each reconstructed muscle group of the caudal series MB.R.2921 of the Late Jurassic sauropod from Tanzania *Giraffatitan* in CNP and CNPs.

		ONP	CNP_2.5%	CNP_5%	CNP_10%	CNP_15%	CNP_20%
Volume (l)							
Muscle	TSP	22.669	20.802	21.312	22.325	23.340	24.354
	LC	76.924	70.681	72.407	75.853	79.303	82.750
	IIC	121.276	114.303	117.115	122.738	128.359	133.982
	IICmed	10.139	9.235	9.451	9.885	10.319	10.753
	CFB	36.952	35.003	35.406	36.213	37.018	37.825
	CFL	170.262	156.311	159.894	167.583	175.097	182.611
	TRPR	9.923	8.972	9.210	9.684	10.159	10.633
	Total	448.144	415.307	424.795	444.281	463.595	482.908
Mass (Kg)							
Muscle	TSP	24.029	22.050	22.591	23.665	24.740	25.815
	LC	81.539	74.922	76.751	80.404	84.061	87.715
	IIC	128.553	121.161	124.142	130.102	136.061	142.021
	IICmed	10.747	9.789	10.018	10.478	10.938	11.398
	CFB	39.169	37.103	37.530	38.386	39.239	40.095
	CFL	180.477	165.690	169.488	177.638	185.603	193.568
	TRPR	10.518	9.510	9.763	10.265	10.769	11.271
	Total	475.032	440.225	450.283	470.938	491.411	511.882

The muscle volumes were calculated with the software Maya. The muscle masses were calculated using the density value proposed by Méndez and Keys (1960) for mammalian muscles (d = 1.06 × 10^3 kg l/m^3). CFB, m. caudofemoralis brevis; CFL, m. caudofermoralis longus; IIC, m. ilioischiocaudalis; IICmed, m. ilioischiocaudalis medial head; LC, m. longissimus caudae; TRPR, m. transversus perinei; TSP, Transversospinalis group. See ***Supplementary Figure S4*** *for the individual segments.*

CNPs

The calculated lengths (from the first caudal vertebra to the last) and masses for the caudal series MB.R.2921 when articulated in the five CNPs are detailed in **Table 2**.

A length difference of 44.76 cm is calculated from the lowest to the highest length values. With our model we suggest that the chosen intervertebral cartilage volume could affect between 14.5 and 17% the total length of the tail. A muscular mass difference of 143.32 kg can be stated between the CNP with the lowest cartilage thickness value (2.5%) and the model with the highest value (20%). With our current model we can hypothesize that the chosen cartilage thickness could affect the total mass of the reconstructed muscles between ca.12 and 14% (ca. 5% when we also take into account the mass of the pelvis and sacrum). The increase of the muscle volumes and masses is proportional to the increase in cartilage thickness ($r^2 = 1$, p-value $< 5.00E-07$) for each muscle individually and all combined (see **Supplementary Table S3**).

TABLE 2 | Total lengths (cm) and masses (kg) calculated for the caudal series MB.R.2921 of the Late Jurassic sauropod from Tanzania *Giraffatitan* in CNP and CNPs.

	Total length	Mass (w/o pelvis)	Mass (w/pelvis)
ONP	280.82	1056.99	2725.74
CNP_2.5%	262.15	987.37	2656.12
CNP_5%	268.55	1007.49	2676.24
CNP_10%	281.34	1048.8	2717.55
CNP_15%	294.12	1089.74	2758.5
CNP_20%	306.91	1130.69	2799.43

DISCUSSION

ONP and CNPs

In light of the steep position of the tail base on the mounted skeleton, a slight upward turn in the distal part of the anterior tail section as suggested for MB.R.2129 is not surprising, seeing how it is required to keep a full tail of ca. 50 vertebrae from dragging on the ground. Overall, the good fit of the alignment with subparallel centra faces and an overall rather straight long axis matches other sauropods and in fact most dinosaurs well (Upchurch et al., 2004). We therefore find no indication that the strong anterior uptilt of the hip of *Giraffatitan* in any major way influenced the overall biomechanical organization of the tail. The total lack of keystoning, already mentioned in relation to overall tail articulation by Janensch (1950a,b) is a marked contrast to e.g., the basal sauropodomorph *Plateosaurus*, in which the addition of chevrons to the digital mount forced a wedge-shaped gap between the caudal vertebral centra that induced a straight tail axis (Mallison, 2010a). Without the chevrons, i.e., with parallel centra faces, the tail of *Plateosaurus* would show a significant ventral curvature (Wellnhofer, 1993; Moser, 2003). In *Giraffatitan*, the distance between chevron and vertebra, caused by the articulation process described, is consistent throughout the tail. N.B.: The articulation in the 3D model is noticeably tighter than on the mounted skeleton, where the support rod for the tail runs between centra and chevrons, making an anatomically correct articulation impossible.

A curvature similar to that seen in MB.R.3736 is also discernible in the hypothetical caudal vertebral series of the titanosaurian sauropod *Lirainosaurus* (Vidal and Díez Díaz, 2017).

However, MB.R.3736 is noticeably straighter, probably because of the articulation morphology between the caudal vertebrae. *Lirainosaurus* has highly procoelous caudal vertebrae, with anterior and posterior articular surfaces highly inclined (*keystoned* centra, see Vidal and Díez Díaz, 2017, fig. 6B).

When comparing the calculated values for the ONP and the CNPs, it can be observed that the most similar lengths and masses are obtained for the ONP and the CNP with an intervertebral cartilage thickness of 10% of the centrum length.

Taylor (2009) calculated a volume of 1520 liters (∼1216 kg, although bone and muscle densities cannot be separated from these calculations) for the tail of *Giraffatitan*, after a modified reconstruction of Paul (1988). Most of the mass of the tail was probably located at its base, where the largest parts of the muscles are placed together with the heaviest bones. It is therefore reasonable to suggest that in *Giraffatitan* at least half of the weight of the tail would have been placed in the first 20 caudal vertebrae. When following our reconstruction and results, the tail of *Giraffatitan* could have weighted ca. 2500 kg (not including the pelvis and sacrum), doubling Taylor's calculations.

Reconstruction of the *Mm. caudofemorales*

The development of the *Mm. caudofemorales*, especially the *M. caudofemoralis longus,* has always been a major issue when reconstructing the tails of extinct animals. The general morphology of the *Mm. caudofemorales* (as well as their origins and insertions) seems to be highly conservative within crocodilians (see e.g., Gatesy, 1991a; Ibiricu et al., 2014). Previous studies suggested that in crocodilians the *M. caudofemoralis longus* originates from the sides of the centrum and ventral surface of the transverse processes of caudal vertebrae 3–15 (Romer, 1923; Galton, 1969). However, Wilhite (2003) confirmed that this muscle additionally originates from the lateral surface of the first 13 chevrons, but only runs along the underside of the transverse processes, from which it is separated by a layer of connective tissue and, in well-fed individuals, by a layer of fat. Therefore, chevron morphology may be indicative of the size, shape, and extent of *M. caudofemoralis longus* in fossil archosaurs. This hypothesis is also followed by Otero and Vizcaíno (2006, 2008). The development and morphology of the transverse processes and the lateral and ventral surfaces of the centra are therefore important indicators for the size, shape and extent of *M. caudofemoralis longus* in sauropod dinosaurs. Several previous studies highlight the importance of the lateroventral surfaces of the anterior caudal centra for the origin and development of the *Mm. caudofemorales* in titanosaurian sauropods (Borsuk-Bialynicka, 1977; Salgado and García, 2002; Salgado et al., 2005), and Gallina and Otero (2009) suggest that the development of the *M. caudofemoralis brevis* and *M. caudofemoralis longus* occurs in relation with the anterior caudal transverse processes morphological variation along the tail. Several osteological correlates are indicative of the development and extent of the *M. caudofemoralis longus* in *Giraffatitan*:

The transverse processes disappear by caudal 25 in MB.R.3736. However, the absence of transverse processes cannot be used for determining the distal end of the *M. caudofemoralis longus*. Persons and Currie, 2011 found that the process expands beyond the distal end of the *M. caudofemoralis longus* in some squamates. In *Alligator mississippiensis* the *M. caudofemoralis longus* ends at the fourteenth caudal vertebra, the first one without transverse processes (Frey, 1988; Mallison, 2019).

- The ventrolateral surfaces of the centra appear from the third to the fourteenth caudal in MR.2921.
- The dorsolateral rugosity is present from chevrons 4 to 11 (caudal vertebrae fifth to twelfth).

Therefore, we inferred the extent of the *M. caudofemoralis longus* from the first caudal vertebra onward and not beyond the fifteenth caudal vertebra in *Giraffatitan*. While the maximal extent of the *M. caudofemoralis longus* is important for volume calculation (and thus maximal force estimates) the bulk of the muscle is located in the anterior region, thus the influence of a slightly longer or shorter muscle (±1 vertebra) are only minor on the total volume. However, a correct reconstruction of *M. transversus perinei* is more important for an accurate estimate of hip joint moments than an exact determination of the taper point of *M. caudofemoralis longus*. The *M. transversus perinei* acts as a lateral constraint on the *M. caudofemoralis longus*. If no *M. transversus perinei* is reconstructed, there is a high risk of overestimation of the *M. caudofemoralis longus* volume at is base, where even minimal changes to the lateral extent induce large volume changes, and accordingly a misestimation of its overall power.

In basal saurischians (e.g., *Eoraptor* and *Guaibasaurus*) and non-avian theropods the *M. caudofemoralis brevis* originates from the brevis fossa, a transitional structure located on the ventromedial surface of the ilium (Carrano and Hutchinson, 2002; Holtz and Omólska, 2004; Langer, 2004; Makovicky and Norell, 2004; Makovicky et al., 2004; Norell and Makovicky, 2004; Omólska et al., 2004; Tykoski and Rowe, 2004). However, in sauropods the origin of the *M. caudofemoralis brevis* is somewhat ambiguous, as they lack a brevis shelf and fossa (Upchurch et al., 2004), similar to the condition in extant crocodilians. In *Giraffatitan* a concave surface appears medially in the postacetabular process, below the last sacral rib and in the junction with the ilium. This surface is inferred as the origin of the *M. caudofemoralis brevis*, in combination with the anterior lateral surface of the centra of caudal vertebra 1 to 3.

The *Mm. caudofemorales* insert on the fourth trochanter of the femur. In sauropods the trochanter appears as a longitudinal ridge, without any differential sites for the insertion of both *M. caudofemoralis longus* and *brevis*. Otero and Vizcaíno (2008) went as far as suggesting a common tendon for both muscles. In the case of *Giraffatitan* the trochanteric ridge is well-developed; therefore, we modeled the insertion of each muscle separately, the *M. caudofemoralis longus* medially and the *M. caudofemoralis brevis* posterolaterally located to the fourth trochanter. In extant crocodiles the insertion is often highly complex, with the tendon of the longus portion wrapping around the very short tendon of the brevis portion, and often inserting into it (Allen, 2015; HM, 2017). However, this complexity leaves no trace on

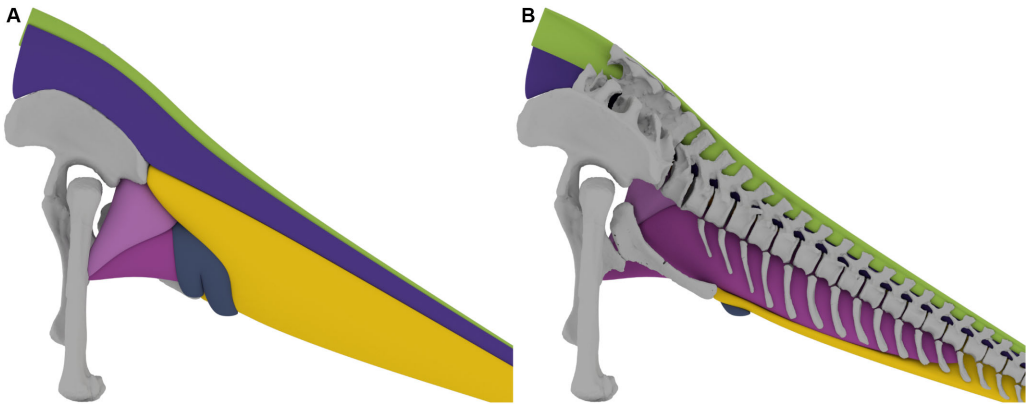

FIGURE 5 | (A) 3D tail muscle reconstruction of the Late Jurassic sauropod *Giraffatitan brancai*. **(B)** Sagittal section of the tail musculature, showing the dorsal and ventral extent of the musculature in relation to the vertebrae.

the bone, so that the exact paths and interactions cannot be reconstructed reliably.

Extent of the Caudal Musculature (Figures 5, 6)

The three-dimensional approach enabled the inference of the size and the spatial arrangement of the musculature. Individual muscles are not only constrained by their origins and insertions, but also by the neighboring musculature. It is therefore insufficient to model only the tail muscles. Consequently the nearby limb musculature was also modeled and taken into account. Nevertheless, some uncertainties regarding the development and proportions, lengths and volumes of the caudal musculature remain. In particular the ventral, lateral and dorsal extensions of the muscles are difficult to reconstruct, e.g., Persons (2009), Persons and Currie (2011), and Mallison (2011) demonstrated that the soft tissues in the tails of crocodilians and many squamates extend significantly beyond the bones dorsally and especially ventrally and laterally. Previous studies on caudal musculature in dinosaurs have predominantly used the extent of the bones as the extension for their soft tissue reconstructions (Carpenter et al., 2005, fig. 17.5; Arbour, 2009, fig. 9; Hutchinson et al., 2011, fig. 5), however, this minimal extension does not appear in any living animal. Persons (2009) correctly pointed out that the lateral width of the transverse processes is often a poor indicator of the lateral extent of *M. caudofemoralis longus* across a wide range of reptiles. Lacertilians such as the leopard gecko (*Eublepharis macularius*), the tokay gecko (*Gekko gecko*) and the green anole (*Anolis carolinensis*) possess tail muscles that extend beyond the bones (Ritzman et al., 2012; Gilbert et al., 2013, fig. 1.B; Sanggaard et al., 2012, fig.2.C, SI Movie_S2). In these lizards, and in the crocodilian *Alligator mississippiensis* (see Frey, 1988; Mallison, 2011) the hypaxial muscles are greatly expanded ventrally and laterally.

The lateral extent of the ventral muscles, the *M. caudofemoralis longus* and the *M. ilioischiocaudalis*, in the mid-tail region of *Giraffatitan* was determined in comparison with the extant crocodilian *Alligator mississippiensis* and in analyzing the general trajectory of these muscles. As muscles are normally not arbitrarily constrained in width by other soft-tissue, it was assumed that they follow a straight line from the origin to the insertion and not in a concave trajectory. In the proximal region the *M. caudofemoralis longus* is constrained in all directions. Medially it is confined by the muscles originating on the ischium, namely the *Mm. adductores femores* and the *M. flexor tibialis internus 3*. The *Mm. adductores femores* originate on the obturator plate and the middle ischial shaft, for *M. adductor femoralis 1* and *M. adductor femoralis 2*, respectively. They run down medially on the hindlimb and insert on the posterior surface of the femur distal to the fourth trochanter. The *Mm. adductores femores* are laterally covered by the *M. flexor tibialis internus 3*, which originates on a shallow depression on the proximal lateral ischium and inserts on the proximal tibia, and runs between the *Mm. adductores femores* and the *M. caudofemoralis longus*, thus limiting the latter medially. Dorsally and laterally the *M. caudofemoralis brevis* wraps around the *M. caudofemoralis longus*, and thus limits the extent in these directions. The *M. caudofemoralis longus* is further constrained laterally by the *M. flexor tibialis externus*, which spans from the postacetabulur process of the ilium to the proximal tibia and restricts both *M. caudofemoralis longus* and *M. caudofemoralis brevis*. Ventrally the *M. caudofemoralis longus* is constrained by the *M. ilioischiocaudalis* and the *M. transversus perinei*, as both encompass *M. caudofemoralis longus* and insert on the distal ischium, thus preventing a ventral extent below the distal tip of the ischium, see **Figure 5**.

In *Alligator mississippiensis*, the *M. tendinoarticularis* is only mildly developed in the tail base, corresponding to an increase in cross section of *M. longissimus caudae* (Frey, 1988). Because of the lack of osteological correlates for the contact between the two muscles any reconstruction must remain speculative, and this relative thinning of the *M. tendinoarticularis* compared to *M. longissimus caudae* has not been represented in previous muscle volume modeling attempts (e.g., Arbour, 2009; Persons, 2009; Persons and Currie, 2011; Persons et al., 2014). However, in the caudal series of *Giraffatitan*, the lateral oblique bulge between the prezygapophysis and the transverse

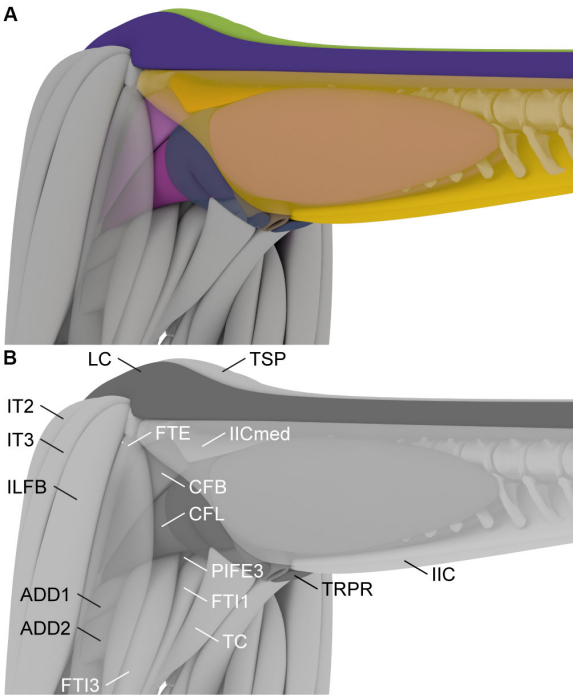

FIGURE 6 | 3D reconstruction of the tail and hindlimb musculature of the Late Jurassic sauropod *Giraffatitan brancai* used to constrain the extent of the *Mm. caudofemorales* muscles. The *m. ilioischiocaudalis* and *m. flexor tibialis externus* are semi-transparent to show the underlying musculature. In color **(A)** and labeled **(B)**. ADD1, *m. adductor femoris 1*; ADD2, *m. adductor femoris 2*; CFB, *m. caudofemoralis brevis*; CFL, *m. caudofemoralis longus*; FTE, *m. flexor tibialis externus*; FTI1, *m. flexor tibialis internus 1*; FTI3, *m. flexor tibialis 3*; IIC, *m. ilioischiocaudalis*; IICmed, *m. ilioischiocaudalis* medial head; IT2, *m. iliotibialis 2*; IT3, *m. iliotibialis 3*; ILFB, *m. iliofibularis*; LC, *m. longissimus caudae*; TC, *m. truncocaudalis*; TRPR, *m. transversus perinei*; TSP, Transversospinalis group.

process (the inferred osteological correlate for the insertion of the *M. tendinoarticularis*) becomes more prominent from the seventh vertebra onward (**Supplementary Figure S3**), disappearing again in the seventeenth caudal vertebra, which formed the basis for the reconstruction and proportions of both the *M. tendinoarticularis* and the *M. longissimus caudae*, confirming that the *M. tendinoarticularis* was less developed at the base of the tail. However, the tendons and fascicles of the epaxial musculature are highly intertwined and thus muscle divisions are not easily distinguishable (e.g., Frey et al., 1989; Tsuihiji, 2005; Organ, 2006; Schwarz-Wings et al., 2009). In our model we simplified the epaxial musculature by only modeling two elements: one gathering all the dorsomedial muscles (the deep musculature, the *M. multifidus,* and the Transversospinalis group), and the lateral *M. longissimus caudae*. However, for biomechanical analyses, and considering all the osteological correlates, individual musculo-tendon units are easier to create and model.

As indicated above, the lateral, ventral and dorsal extent of the tail is difficult to estimate in extinct animals. The base of the tail is laterally delimited for three main muscles: dorsally by the *M. longissimus caudae*, and ventrally by the dorsal ramus of the *M. ilioischiocaudalis* and the lateral expansion of the *M. caudofemoralis brevis*. Anatomically, and in terms of volume, the *M. longissimus caudae* (epaxial), the *M. caudofemoralis* group and the *M. ilioischiocaudalis* (hypaxial) seem to be the most important muscles of the base of the tail. Then, from the fifth caudal vertebra, when both rami of the *M. ilioischiocaudalis* meet and totally enclose the *M. caudofemoralis longus*, all the muscular groups occupy similar volumes.

Internal Structure of Epaxial Muscles

While we propose that the suite of epaxial and hypaxial tail muscles of *Giraffatitan*, including the *Mm. caudofemorales*, are generally comparable in terms of its general extensions, origins and insertions to crocodilians, here are some key differences between extant archosaurs and our inference for the tail musculature in *Giraffatitan*. Extant crocodilians possess a very specialized internal muscle architecture (e.g., Frey, 1988; Salisbury and Frey, 2001). Whereas the medial epaxial muscles, in particular *M. multifidus*, *M. spinalis*, and *M. articulospinalis*, form a system of counter-running (criss-crossing) tendons, the lateral epaxial muscles *M. tendinoarticularis* and in particular *M. longissimus* form large myoseptal sheets and cones. The tendons of the epaxial muscles are connected firmly not only to the vertebrae, but also to the osteoderms. The close association between the myosepts and tendons of the epaxial muscles in crocodilians is important as it forms a part of their bracing system (Salisbury and Frey, 2001). Besides, in contrast to extant birds and sauropods, extant and fossil crocodilians do not possess postcranial skeletal pneumaticity (e.g., Gower, 2001).

Additionally, birds also have a highly modified internal muscular construction, and thus their anatomy cannot simply be extrapolated onto non-avian dinosaurs. In birds, the presacral epaxial muscles form muscles slips that attach only to small areas of the bone (e.g., Boas, 1929; Zweers et al., 1987; Vanden Berge and Zweers, 1993). In combination with that, extant bird skeletons are highly pneumatic, which means that the vertebrae are interspersed by a large number of pneumatic diverticula that occupy parts of the vertebral surface and additionally resolve the vertebral surface to create pneumatic foramina (Gier, 1952; Duncker, 1971; Hogg, 1984a; Witmer, 1997; O'Connor, 2004), and muscle attachment areas are generally small.

For sauropod dinosaurs, a similar slip-like internal muscular architecture of the epaxial muscles as in extant birds has been hypothesized, based on the presence of unambiguous osteological correlates at the presacral vertebrae (see Wedel and Sanders, 2002; Taylor and Wedel, 2013b). Another similarity to birds is the presence of vertebral pneumaticity at least in the presacral vertebral column of most neosauropods (Wedel, 2003a,b, 2009); and additionally saltasaurine titanosaurs possess pneumatic sacral and anterior caudal vertebrae (Cerda et al., 2012; Zurriaguz and Cerda, 2017).

These similarities and differences need to be kept in mind when reconstructing the internal structure of musculature of non-avian dinosaurs. However, our model is a simplification, and

the reconstruction of the detailed internal muscle architecture is beyond the scope of this study.

Caudal Skeletal Pneumaticity and Its Influence on the Musculoskeletal System

Caudal pneumaticity is widely present in Neosauropoda, like the camellate internal tissue of titanosaurs. More basal titanosauriforms, as *Lusotitan* (Mannion et al., 2013; Mocho et al., 2017) and *Giraffatitan* (Wedel and Taylor, 2013), also present caudal pneumatic features, as lateral fossa and foramina. This caudal skeletal pneumaticity is also present in other sauropods, like *Apatosaurus*, *Barosaurus*, *Diplodocus*, *Tastavinsaurus,* and *Tornieria* (McIntosh, 2005; Remes, 2006; Royo-Torres, 2009; Mannion et al., 2013) [for more neosauropods with caudal skeletal pneumaticity see **Table 1** of Wedel and Taylor (2013)]. When diagnosing a fossa as pneumatic, is useful to check other pneumatic features on the same bone (Wedel, 2005; O'Connor, 2006), but also observe the presence of pneumatic foramina and subfossa within the fossa (Wilson, 1999; Yates et al., 2012). However, the interaction between air sacs and muscle development has not been studied in detail.

Caudal pneumaticity has been previously described in the three caudal series of *Giraffatitan* (Wedel and Taylor, 2013). This work describes with high detail all the pneumatic structures, so here we will only address the main features that could be useful for the musculoskeletal reconstruction of the tail of *Giraffatitan*.

MB.R.5000 caudal series presents the most complex pattern of pneumatization within Dinosauria (see Wedel and Taylor, 2013, fig. 8), but, as previously stated, MB.R.5000 could not be analyzed in our study. However, these characters are very useful when identifying and describing the ones present in the other caudal series from *Giraffatitan*. Several hypotheses were made related to the different extension of caudal pneumatization between MB.R.5000 and the other 2 caudal series referred to *Giraffatitan* (see Wedel and Taylor, 2013, and references herein). We followed the hypothesis of intraspecific variation, and used the pneumatic features of the series MB.R. 2921 and 3736 for our reconstruction. We confirmed Wedel and Taylor (2013) observation, that small pneumatic fossa are present on both sides of the centrum, below the transverse processes, in the second caudal of the series MB.R.2921 and MB.R.3736, whereas the rest of the caudal vertebrae of the series is apneumatic. These pneumatic diverticula (cryptic diverticula) also appear on extant birds and pterosaurs, and do not leave any diagnostic skeletal traces. The posterior dorsal vertebrae, synsacrum, pelvic girdle and hindlimb of birds are pneumatized by diverticula of the abdominal air sacs (Cover, 1953; King, 1966, 1975; Duncker, 1971; Hogg, 1984a,b; Bezuidenhout et al., 1999; O'Connor and Claessens, 2005; O'Connor, 2006). In the case of *Giraffatitan*, the caudal vertebral diverticula most plausibly originated from abdominal air sacs too, as also hypothesized by Wedel et al. (2000) and Wedel (2009) for the pneumatization of postdorsal vertebrae in non-avian dinosaurs.

In extant birds pneumatic diverticula have different ways of distribution, they pass along under the skin, in between the muscles, and among the viscera, and only a few of them leave traces on the skeleton (Duncker, 1971). However, these intermuscular diverticula are highly difficult to assess in extinct species. Although we have evidence of pneumatic features in the proximal part of the caudal series of *Giraffatitan* we have not included reconstructions of the caudal pneumatic diverticula, as they do not have a huge impact on the final extension of the muscular system.

Functions of the Caudal Muscle Systems

Epaxial Musculature

This complex of muscles has its major importance in the stabilization of all the vertebral column and equally in the flexion of parts of the vertebral column (Alexander, 1985; Salisbury and Frey, 2001; Henderson, 2004; Schwarz-Wings, 2009). Especially, the deep musculature and the *M. multifidus* help in this stabilization and, by synchronous contraction, in the dorsal bending of the tail, by connecting the apical edges of the neural spines. Lateral flexion of the tail is achieved by synchronous ipsilateral contraction of the *M. transversospinalis* Group, the *M. longissimus caudae* and/or the *M. ilioischiocaudalis*).

Hypaxial Musculature

The *M. caudofemoralis longus* (together with the *M. caudofemoralis brevis*) is the main hindlimb retractor in diapsids. It adducts and longitudinally rotates the femur (e.g., Gatesy, 1991a). The *M. caudofemoralis longus* is correlated with the *M. ilioischiocaudalis*: while the former is contracted, the *M. ilioischiocaudalis* (together with the epaxial *M. transversospinalis* Group and the *M. longissimus caudae*) help to stabilize the tail base to prevent unwanted movement of the tail by the *M. caudofemoralis longus*. *M. transversus perinei* wraps the *M. caudofemoralis longus* and thereby has a direct effect by limiting its maximum cross-section, which then has the effect of specifying more precisely the moment arm of this muscle. Additional quantitative biomechanical studies are needed to test this hypothesis.

CONCLUSION

We created a detailed three-dimensional musculoskeletal reconstruction of approximately the anterior half of the tail of the Late Jurassic sauropod *Giraffatitan brancai*, based on comparative anatomy, primarily with crocodilians, and digital techniques, such as photogrammetry and an innovative three-dimensional modeling approach. Using this reconstruction we were able to calculate the mass of the individual elements and hypothesize a total mass of ca. 2500 kg for the complete tail. We further suggest, based on our assessment of the musculoskeletal reconstruction, that *Giraffatitan* had a powerful tail that assisted in its stabilization, and propulsion, but also as counterweight for the presacral part of the body. The suite of hypaxial and epaxial muscles fulfills an important role in stabilizing the tail and hold it over the ground by synchronous bilateral contraction to optimize the moment arms for the main hindlimb retractor muscles, the *M. caudofemoralis longus*. Although *Giraffatitan* had a short tail

(compared to other concurrent taxa, e.g., diplodocids and other coexisting macronarians), it was well-developed and robust.

Additionally, we were able to confirm that Janensch (1950b) was right in his original assessment of the tail posture, and the current mount at the Museum für Naturkunde, after the remounting in 2007 when the skeleton was mounted adapting the resting posture of the animal based on the current knowledge on the anatomy and biomechanics of sauropods (Remes et al., 2011), is correct.

Intervertebral cartilage thickness is difficult to assess in extinct taxa. In this work we have observed that similar values for tail length and muscle masses and volumes are calculated for the MB.R.2129 caudal series of *Giraffatitan* both in ONP and in CNP with a cartilage thickness of 10%. Taylor (2014) also suggested 10% as best estimate for cartilage thickness for the neck of *Diplodocus* and *Apatosaurus*. And as previously stated by Christian and Preuschoft (1996) and Christian and Dzemski (2007), the zygapophyseal articulation overall probably reflects the intervertebral cartilage volume, which as seen could be ca. 10% of the centrum length. We agree with Taylor (2014), and suggest using a cartilage thickness between 10 and 15% when reconstructing sauropod axial series.

The methodology applied in this study helps us to better comprehend the biomechanical and detailed anatomical aspects of a reconstructed musculoskeletal system of an extinct animal and, in addition, to estimate the volume and mass more accurately.

DATA AVAILABILITY STATEMENT

All created 3D models and derived files of this study are stored in MorphoSource (project ID: 000664927) under CC-BY-NC license and are freely available under the following link: https://www.morphosource.org/projects/000664927?locale=en. Further inquiries can be directed to the corresponding author.

AUTHOR CONTRIBUTIONS

VD, DS, and HM conceived and designed the study. VD and HM digitized the specimens. VD and OD performed the data analyses. OD performed the 3D modeling and prepared the figures. All authors contributed to the interpretation of the data, writing of the manuscript, read and approved the submitted version.

FUNDING

This study was supported by the Alexander von Humboldt Stiftung provided for VD.

ACKNOWLEDGMENTS

Mathew J. Wedel (Western University of Health Sciences in Pomona, California) provided useful help and comments on the postcranial skeletal pneumaticity. We would also like to thank the editor PR and the two reviewers PF and RT, who improved this work with their comments and suggestions.

SUPPLEMENTARY MATERIAL

The Supplementary Material for this article can be found online at: https://www.frontiersin.org/articles/10.3389/feart.2020.00160/full#supplementary-material

REFERENCES

Alexander, R. M. (1985). Mechanics of posture and gait of some large dinosaurs. *Zool. J. Linn. Soc. Lond.* 83, 1–25.

Allen, V., Molnar, J., Parker, W., Pollard, A., Nolan, G., and Hutchinson, J. R. (2014). Comparative architectural properties of limb muscles in Crocodylidae and Alligatoridae and their relevance to divergent use of asymmetrical gaits in extant Crocodylia. *J. Anat.* 225, 569–582. doi: 10.1111/joa.12245

Allen, V. R. (2010). *The Evolution of the Avian Hindlimb Conformation and Locomotor Function*. Ph.D. thesis, The Royal Veterinary College, London.

Arbour, V. M. (2009). Estimating impact forces of tail club strikes by ankylosaurid dinosaurs. *PLoS One* 4:e6738. doi: 10.1371/journal.pone.0006738

Bezuidenhout, A. J., Groenewald, H. B., and Soley, J. T. (1999). An anatomical study of the respiratory air sacs in ostriches. *Onderstepoort J. Vet. Res.* 66, 317–325.

Boas, J. E. V. (1929). *Biologisch-Anatomische Studien Über den Hals der Vögel. D. Kgl. Danske Vidensk. Selsk. skrifter: Naturvidensk. og Mathem. Afd*, Vol. 9. Copenhagen: Høst & Søn, 122.

Borsuk-Bialynicka, M. (1977). A new camarasaurid sauropod *Opisthocoelicaudia skarzynskii*, gen. n. sp. n. from the Upper Cretaceous of Mongolia. *Palaeontol. Polon.* 37, 45–64.

Bryant, H. N., and Russell, A. P. (1992). The role of phylogenetic analysis in the inference of unpreserved attributes of extinct taxa. *Philos. Trans. R. Soc. Lond. B* 337, 405–418.

Button, D. J., Barrett, P. M., and Rayfield, E. J. (2016). Comparative cranial myology and biomechanics of *Plateosaurus* and *Camarasaurus* and evolution of the sauropod feeding apparatus. *Palaeontology* 59, 887–913.

Carballido, J. L., Pol, D., Parra Ruge, M. L., Padilla Bernal, S., Páramo-Fonseca, M., and Etayo-Serna, F. (2015). A new early cretaceous brachiosaurid (Dinosauria, Neosauropoda) from northwestern Gondwana (Villa de Leiva, Colombia). *J. Vertebr. Paleontol.* 35:e980505. doi: 10.1080/02724634.2015.980505

Carballido, J. L., and Sander, P. M. (2014). Postcranial axial skeleton of *Europasaurus holgeri* (Dinosauria, Sauropoda) from the Upper Jurassic of Germany: implications for sauropod ontogeny and phylogenetic relationships of basal Macronaria. *J. Syst. Palaeontol.* 12, 335–387.

Carpenter, K., Sanders, F., McWhinney, L. A., and Wood, L. (2005). "Evidence for predator-prey relationships. Examples for *Allosaurus* and *Stegosaurus*," in *The Carnivorous Dinosaurs*, ed. K. Carpenter (Bloomington, IN: Indiana University Press), 325–350.

Carrano, M. T., and Hutchinson, J. R. (2002). Pelvic and hindlimb musculature of *Tyrannosaurus rex* (Dinosauria: Theropoda). *J. Morphol.* 253, 207–228. doi: 10.1002/jmor.10018

Cerda, I. A., Salgado, L., and Powell, J. E. (2012). Extreme postcranial pneumaticity in sauropod dinosaurs from South America. *Paläontol. Z.* 86, 441–449.

Christian, A., and Dzemski, G. (2007). Reconstruction of the cervical skeleton posture of *Brachiosaurus brancai* Janensch, 1914 by an analysis of the intervertebral stress along the neck and a comparison with the results of different approaches. *Fossil Record* 10, 38–49.

Christian, A., and Preuschoft, H. (1996). Deducing the body posture of extinct large vertebrates from the shape of the vertebral column. *Palaeontology* 39, 801–812.

Cong, L., Hou, L., Wu, X., and Hou, J. (1998). *The Gross Anatomy of Alligator Sinensis* Fauvel. Beijing: Forestry Publishing House.

Coria, R., Filippi, L. S., Chiappe, L. M., García, R., and Arcucci, A. B. (2013). *Overosaurus paradasorum* gen. et sp. nov., a new sauropod dinosaur (Titanosauria: Lithostrotia) from the late cretaceous of Neuquén, Patagonia, Argentina. *Zootaxa* 3683, 357–376. doi: 10.11646/zootaxa.3683.4.2

Cott, H. B. (1961). Scientific results of an inquiry into the ecology and economic status of the Nile crocodile (*Crocodylus niloticus*) in Uganda and northern Rhodesia. *Trans. Zool. Soc. Lond.* 229, 211–236.

Cover, M. S. (1953). Gross and microscopic anatomy of the respiratory system of the turkey. III. The air sacs. *Am. J. Vet. Res.* 14, 239–245.

Cunningham, J. A., Rahman, I. A., Lautenschlager, S., Rayfield, E. J., and Donoghue, P. C. J. (2014). A virtual world of paleontology. *Trends Ecol. Evol.* 29, 347–357. doi: 10.1016/j.tree.2014.04.004

Dececchi, T. A., and Larsson, H. C. (2013). Body and limb size dissociation at the origin of birds: uncoupling allometric constraints across a macroevolutionary transition. *Evolution* 67, 2741–2752. doi: 10.1111/evo.12150

Dilkes, D. (1999). Appendicular myology of the hadrosaurian dinosaur *Maiasaura peeblesorum* from the Late Cretaceous (Campanian) of Montana. *Earth Environ. Sci. Trans. R. Soc.* 90, 87–125.

Duncker, H.-R. (1971). The lung air sac system of birds. *Adv. Anat. Embryol. Cell Biol.* 45, 1–171. doi: 10.1017/S1464793106007111

Fahlke, J. M., and Autenrieth, M. P. (2016). photogrammetry vs. Micro-CT scanning for 3D surface generation of a typical vertebrate fossil – a case study. *J. Paleontol. Tech.* 14, 1–18.

Fletcher, J. W. A., Williams, S., Whitehouse, M. R., Gill, H. S., and Preatoni, E. (2018). Juvenile bovine bone is an appropriate surrogate for normal and reduced density human bone in biomechanical testing: a validation study. *Sci. Rep.* 8:10181. doi: 10.1038/s41598-018-28155-w

Frey, E. (1982a). Der Bau des Bewegungsapparates der Krokodile und seine Funktion bei der aquatischen Fortbewegung. Diploma thesis, University of Tübingen: Facultät Biologie, p. 204.

Frey, E. (1982b). Ecology, locomotion, and tail muscle anatomy of crocodiles. *Neues Jahrb. Geol. Paläontol. Abh.* 164, 194–199.

Frey, E. (1988). Anatomie des Körperstammes von *Alligator mississippiensis* Daudin (Anatomy of the body stem of *Alligator mississippiensis* Daudin). *Stuttg. Beitr. Nat. Ser. A* 424, 1–106.

Frey, E., Riess, J., and Tarsitano, S. F. (1989). The axial tail musculature of recent crocodiles and its phyletic implications. *Am. Zool.* 29, 857–862.

Gallina, P. A., and Otero, A. (2009). Anterior caudal transverse processes in sauropod dinosaurs: morphological, phylogenetic and functional aspects. *Ameghiniana* 46, 165–176.

Galton, P. M. (1969). The pelvic musculature of the dinosaur *Hypsilophodon* (Reptilia: Ornithischia). *Postilla* 131:64.

Gatesy, S. M. (1991a). Caudofemoral musculature and the evolution of theropod locomotion. *Paleobiology* 16, 170–186. doi: 10.1371/journal.pone.0025763

Gatesy, S. M. (1991b). Hind limb movements of the American alligator (*Alligator mississippiensis*) and postural grades. *J. Zool. Lond.* 224, 577–588.

Gatesy, S. M., and Dial, K. P. (1996). From frond to fan: *Archaeopteryx* and the evolution of short-tailed birds. *Evolution* 50, 2037–2048. doi: 10.1111/j.1558-5646.1996.tb03590.x

Gier, H. T. (1952). The air sacs of the loon. *Auk* 69, 40–49.

Gignac, P. M. and Erickson, G. M. (2017). The Biomechanics Behind Extreme Osteophagy in *Tyrannosaurus rex*. *Sci. Rep.* 7:2012. doi: 10.1038/s41598-017-02161-w

Gilbert, E. A. B., Payne, S. L., and Vickaryous, M. K. (2013). The anatomy and histology of caudal autotomy and regeneration in lizards. *Physiol. Biochem. Zool* 86, 631–644. doi: 10.1086/673889

Gilmore, C. (1925). A nearly complete articulated skeleton of *Camarasaurus*, a saurischian dinosaur from the Dinosaur National Monument. *Mem. Carnegie Mus.* 10, 347–384.

Gower, D. J. (2001). Possible postcranial pneumaticity in the last common ancestor of birds and crocodilians: evidence from *Erythrosuchus* and other Mesozoic archosaurs. *Naturwissenschaften* 88, 119–122. doi: 10.1007/s001140100206

Hair, P. (1868). On the arrangement of the muscular fibers of the alligator. *J. Anat.* 2, 26–41.

Henderson, D. M. (2004). Axial stress as a growth constraint in the vertebrae of sauropod dinosaurs. *J. Morphol.* 260, 297.

Hogg, D. A. (1984a). The development of pneumatisation in the skeleton of the adult domestic fowl. *J. Anat.* 139, 105–113.

Hogg, D. A. (1984b). The distribution of pneumatisation in the skeleton of the adult domestic fowl. *J. Anat.* 138, 617–629.

Holtz, T. R. Jr., and Omólska, H. (2004). "Saurischia," in *The Dinosauria*, 2nd Edn, eds D. B. Weishampel, P. Dodson, and H. Osmólska (Berkeley, CA: University of California Press), 21–24.

Hutchinson, J. R. (2002). The evolution of hindlimb tendons and muscles on the line to crown-group birds. *Comp. Biochem. Physiol. Part Mol. Integr. Physiol.* 133, 1051–1086. doi: 10.1016/s1095-6433(02)00158-7

Hutchinson, J. R., Bates, K. T., Molnar, J., Allen, V., and Makovicky, P. J. (2011). A computational analysis of limb and body dimensions in *Tyrannosaurus rex* with implications for locomotion, ontogeny, and growth. *PLoS One* 6:e26037. doi: 10.1371/journal.pone.0026037

Hutchinson, J. R., Felkler, D., Houston, K., Chang, Y. M., Brueggen, J., Kledzik, D., et al. (2019). Divergent evolution of terrestrial locomotor abilities in extant Crocodylia. *Sci. Rep.* 9:19302. doi: 10.1038/s41598-019-55768-6

Hutchinson, J. R., and Gatesy, S. M. (2000). Adductors, abductors, and the evolution of archosaur locomotion. *Paleobiology* 26, 734–751.

Hutchinson, J. R., Rankin, J. W., Rubenson, J., Rosenbluth, K. H., Siston, R. A., and Delp, S. L. (2015). Musculoskeletal modelling of an ostrich (*Struthio camelus*) pelvic limb: influence of limb orientation on muscular capacity during locomotion. *PeerJ* 3:e1001. doi: 10.7717/peerj.1001

Ibiricu, L. M., Lamanna, M. C., and Lacovara, K. J. (2014). The influence of caudofemoral musculature on the Titanosaurian (Saurischia: Sauropoda) tail skeleton: morphological and phylogenetic implications. *Hist. Biol.* 26, 454–471.

Janensch, W. (1914). Übersicht über die wirbeltierfauna der tendaguruschichten, nebst einer kurzen charakterisierung der neu aufgeführten arten von Sauropoden. *Archiv. Biontol.* 3, 81–110.

Janensch, W. (1950a). Die Wirbelsaule von *Brachiosaurus brancai*. *Palaeontographica* 3(Suppl. 7), 27–93.

Janensch, W. (1950b). Die Skelettrekonstruktion von *Brachiosaurus brancai*. *Palaeontographica* 3(Suppl. 7), 95–102.

Janensch, W. (1961). Die Gliedmaßen und Gliedmaßengürtel der Sauropoden der Tendaguru-Schichten. *Palaeontographica* 3(Suppl. 7), 177–235.

King, A. S. (1966). Structural and functional aspects of the avian lungs and air sacs. *Int. Rev. Gen. Exp. Zool.* 2, 171–267.

King, A. S. (1975). "Aves respiratory system," in *Sisson and Grossman's the Anatomy of the Domestic Animals*, 5th Edn, Vol. 2, ed. R. Getty (Philadelphia, PA: Saunders), 1883–1918.

Lacovara, K. J., Lamanna, M. C., Ibiricu, L. M., Poole, J. C., Schroeter, E. R., Ullmann, P. V., et al. (2014). A gigantic, exceptionally complete titanosaurian sauropod dinosaur from Southern Patagonia, Argentina. *Sci. Rep.* 4:6196. doi: 10.1038/srep06196

Langer, M. C. (2004). "Basal saurischia," in *The Dinosauria*, 2nd Edn, eds D. B. Weishampel, P. Dodson, and H. Osmólska (Berkeley, CA: University of California Press), 25–46.

Lautenschlager, S. (2013). Cranial myology and bite force performance of *Erlikosaurus andrewsi*: a novel approach for digital muscle reconstructions. *J. Anat.* 222, 260–272. doi: 10.1111/joa.12000

Makovicky, P. J., Kobayashi, Y., and Currie, P. J. (2004). "Therizinosauroidea," in *The Dinosauria*, 2nd Edn, eds D. B. Weishampel, P. Dodson, and H. Osmólska (Berkeley, CA: University of California Press), 151–164.

Makovicky, P. J., and Norell, M. A. (2004). "Troodontidae," in *The Dinosauria*, 2nd Edn, eds D. B. Weishampel, P. Dodson, and H. Osmólska (Berkeley, CA: University of California Press), 184–195.

Mallison, H. (2010a). The digital *Plateosaurus* I: body mass, mass distribution and posture assessed using CAD and CAE on a digitally mounted complete skeleton. *Palaeontol. Electron.* 2, 1–26.

Mallison, H. (2010b). The digital *Plateosaurus* II: an assessment of the range of motion of the limbs and vertebral column and of previous reconstructions using a digital skeletal mount. *Acta Palaeontol. Polon.* 55, 433–458.

Mallison, H. (2011). Defense capabilities of *Kentrosaurus aethiopicus* Hennig, 1915. *Palaeontol. Electron.* 14, 1–25.

Mallison, H., Belvedere, M., and Díez Díaz, V. (2017). *3D Imaging Handbook: Photogrammetry Digitization techniques for the SYNTHESYS Project*. Available online at: http://biowikifarm.net/v-mfn/3d-handbook/Photogrammetry_MfN (accessed, 2017).

Mallison, H., and Wings, O. (2014). Photogrammetry in paleontology–a practical guide. *J. Paleontol. Tech.* 12, 1–31.

Mannion, P. D., Upchurch, P., Barnes, R. N., and Mateus, O. (2013). Osteology of the late Jurassic Portuguese sauropod dinosaur *Lusotitan atalaiensis* (Macronaria) and the evolutionary history of basal titanosauriforms. *Zool. J. Linn. Soc.* 168, 98–206.

McIntosh, J. S. (2005). "The genus *Barosaurus* marsh (Sauropoda, Diplodocidae)," in *Thunderlizards. The Sauropodomorph Dinosaurs*, eds V. Tidwell and K. Carpenter (Bloomington, IN: Indiana University Press), 38–77.

Méndez, J., and Keys, A. (1960). Density and composition of mammalian muscle. *Metabolism* 9, 184–188.

Mocho, P., Royo-Torres, R., Malafaia, E., Escaso, F., and Ortega, F. (2017). First occurrences of non-neosauropod eusauropod procoelous caudal vertebrae in the Portuguese Upper Jurassic record. *Geobios* 50, 23–36.

Mohiuddin, S. (2013). Change in bone density as a function of water content. *World J. Med. Sci.* 8, 48–51.

Moser, M. (2003). *Plateosaurus engelhardti* Meyer, 1837 (Dinosauria: Sauropodomorpha) aus dem Feuerletten (Mittelkeuper; Obertrias) von Bayern. *Zittel. Reihe B Abh. Bayer. Staatssammlung Paläontol. Geol.* 24, 3–186.

Norell, M. A., and Makovicky, P. J. (2004). "Dromaeosauridae," in *The Dinosauria*, 2nd Edn, eds D. B. Weishampel, P. Dodson, and H. Osmólska (Berkeley, CA: University of California Press), 196–209.

O'Connor, J., Wang, X., Sullivan, C., Zheng, X., Tubaro, P., Zhang, X., et al. (2013). Unique caudal plumage of *Jeholornis* and complex tail evolution in early birds. *Proc. Natl. Acad. Sci. U.S.A.* 110, 17404–17408. doi: 10.1073/pnas.1316979110

O'Connor, P., and Claessens, L. P. A. M. (2005). Basic avian pulmonary design and flowthrough ventilation in non-avian theropod dinosaurs. *Nature* 436, 253–256. doi: 10.1038/nature03716

O'Connor, P. M. (2004). Pulmonary pneumaticity in the postcranial skeleton of extant Aves: a case study examining Anseriformes. *J. Morphol.* 261, 141–161. doi: 10.1002/jmor.10190

O'Connor, P. M. (2006). Postcranial pneumaticity: an evaluation of soft-tissue influences on the postcranial skeleton and the reconstruction of pulmonary anatomy in archosaurs. *J. Morphol.* 267, 1199–1226. doi: 10.1002/jmor.10470

Omólska, H., Currie, P. J., and Barsbold, R. (2004). "Oviraptorosauria," in *The Dinosauria*, 2nd Edn, eds D. B. Weishampel, P. Dodson, and H. Osmólska (Berkeley, CA: University of California Press), 165–183.

Organ, C. L. (2006). Thoracic epaxial muscles in living archosaurs and ornithopod dinosaurs. *Anat. Rec.* 288A, 782–793. doi: 10.1002/ar.a.20341

Otero, A., and Vizcaíno, S. F. (2006). "Hindlimb musculature of *Neuquensaurus australis* Lydekker (Sauropoda, Titanosauria)," in *Proceedings of the 9th Congreso Argentino de Paleontología y Bioestratigrafía*, (Córdoba: Academia Nacional de Ciencias, Resúmenes), 135.

Otero, A., and Vizcaíno, S. F. (2008). Hindlimb musculature and function of *Neuquensaurus australis* Lydekker (Sauropoda: Titanosauria). *Ameghiniana* 45, 333–348.

Paul, G. S. (1988). The brachiosaur giants of the Morrison and Tendaguru with a description of a new subgenus, *Giraffatitan*, and a comparison of the world's largest dinosaurs. *Hunteria* 2, 1–14.

Persons, W. (2009). Theropod tail muscle reconstruction and assessment of the locomotive contributions of the *M. caudofemoralis*. *J. Vertebr. Paleontol.* 3:164A.

Persons, W., and Currie, P. J. (2011). The tail of *Tyrannosaurus*: reassessing the size and locomotive importance of the *M. caudofemoralis* in non-avian theropods. *Anat. Rec.* 294, 119–131. doi: 10.1002/ar.21290

Persons, W., Currie, P. J., and Norell, M. A. (2014). Oviraptorosaur tail forms and functions. *Acta Palaeontol. Polon.* 59, 553–567.

Persons, W. S., and Currie, P. J. (2012). Dragon tails: convergent caudal morphology in winged archosaurs. *Acta Geol. Sin.* 86, 1402–1412.

Pittman, M., Gatesy, S. M., Upchurch, P., Goswami, A., and Hutchinson, J. R. (2013). Shake a tail feather: the evolution of the theropod tail into a stiff aerodynamic surface. *PLoS One* 8:e63115. doi: 10.1371/journal.pone.0063115

Rahman, I. M., and Lautenschlager, S. (2017). Applications of three-dimensional box modelling to paleontological functional analysis. *Paleontol. Soc. Pap.* 22, 119–132.

Rashid, D. J., Chapman, S. C., Larsson, H. C. E., Organ, C. L., Bebin, A.-G., Merzdorf, C. S., et al. (2014). From dinosaurs to birds: a tail of evolution. *EvoDevo J.* 5:25. doi: 10.1186/2041-9139-5-25

Remes, K. (2006). Revision of the Tendaguru sauropod dinosaur *Tornieria Africana* (Fraas) and its relevance for sauropod paleobiogeography. *J. Vertebr. Paleontol.* 26, 651–669.

Remes, K., Ortega, F., Fierro, I., Joger, U., Kosma, R., Marín Ferrer, J. M., et al. (2009). A new basal sauropod dinosaur from the middle jurassic of niger and the early evolution of sauropoda. *PLoS One* 4:e6924. doi: 10.1371/journal.pone.0006924

Remes, K., Unwin, D. M., Klein, N., Heinrich, W.-D., and Hampe, O. (2011). "Skeletal reconstruction of *Brachiosaurus brancai* in the Museum für Naturkunde, Berlin: summarizing 70 years of sauropod research," in *Biology of the Sauropod Dinosaurs. Understanding the Life of Giants 305-316*, eds N. Klein, K. Remes, C. T. Gee, and P. M. Sander (Bloomington, IN: Indiana University Press).

Ritzman, T. B., Stroik, L. K., Julik, E., Hutschins, E. D., Lasku, E., Denardo, D. F., et al. (2012). The gross anatomy of the original and regenerated tail in the green anole (*Anolis carolinensis*). *Anat. Rec.* 295, 1596–1608. doi: 10.1002/ar.22524

Romer, A. S. (1923). Crocodilian pelvic muscles and their avian and reptilian homologues. *Bull. Am. Mus. Nat. His.* 48, 533–552.

Royo-Torres, R. (2009). El saurópodo de Peñarroya de Tastavins. *Monogr. Turol.* 6, 1–548.

Salgado, L., Apesteguía, S., and Heredia, S. E. (2005). A new specimen of *Neuquensaurus australis*, a late cretaceous saltasaurinae titanosaur from North Patagonia. *J. Vertebr. Paleontol.* 25, 623–634.

Salgado, L., and García, R. (2002). Variación morfológica en la secuencia de vértebras caudales de algunos saurópodos titanosaurios. *Rev. Esp. Paleontol.* 17, 211–216.

Salisbury, S. W., and Frey, E. (2001). "The kinematics of aquatic locomotion in *Osteolaemus tetraspis* Cope," in *Crocodilian Biology and Evolution*, eds G. C. F. Grigg, F. Seebacher, and C. E. Franklin (Chipping Norton, NSW: Surrey Beatty & Sons), 165–179.

Sanggaard, K. W., Danielsen, C. C., Wogensen, L., Vinding, M. S., Rydtoft, L. M., Mortensen, M. B., et al. (2012). Unique structural features facilitate lizard tail autotomy. *PLoS One* 7:e51803. doi: 10.1371/journal.pone.0051803

Schwarz-Wings, D. (2009). Reconstruction of the thoracic epaxial musculature of diplodocid and dicraeosaurid sauropods. *J. Vertebr. Paleontol.* 29, 517–534.

Schwarz-Wings, D., Frey, E., and Martin, T. (2009). Reconstruction of the bracing system of the trunk and tail in hyposaurine dryosaurids (Crocodylomorpha; Mesoeucrocodylia). *J. Vertebr. Paleontol.* 29, 453–472.

Sharp, A. (2014). Three dimensional digital reconstruction of the jaw adductor musculature of the extinct marsupial giant *Diprotodon optatum*. *PeerJ* 2:e514. doi: 10.7717/peerj.514

Stevens, K. A., and Parrish, J. M. (1999). Neck posture and feeding habits of two Jurassic sauropod dinosaurs. *Science* 284, 798–800. doi: 10.1126/science.284.5415.798

Stevens, K. A., and Parrish, M. J. (2005a). "Digital reconstructions of sauropod dinosaurs and implications for feeding," in *The Sauropods: Evolution and Paleobiology*, eds J. A. Wilson and K. Curry Rogers (Berkeley, CA: University of California Press), 178–200.

Stevens, K. A., and Parrish, M. J. (2005b). "Neck posture, dentition and feeding strategies in Jurassic sauropod dinosaurs," in *Thunder Lizards: The Sauropodomorph Dinosaurs*, eds V. Tidwell and K. Carpenter (Bloomington, IN: Indiana University Press), 212–232.

Sutton, M. D., Rahman, I. A., and Garwood, R. J. (2014). *Techniques for Virtual Palaeontology*. Chichester: John Wiley & Sons, 208.

Taylor, M. P. (2009). A re-evaluation of *Brachiosaurus altithorax* Riggs 1903 (Dinosauria, Sauropoda) and its generic separation from *Giraffatitan brancai* (Janensch, 1914). *J. Vertebr. Palaeontol.* 29, 787–806.

Taylor, M. P. (2011). Correction: a re-evaluation of *Brachiosaurus altithorax* Riggs 1903 (Dinosauria, Sauropoda) and its generic separation from *Giraffatitan brancai* (Janensch, 1914). *J. Vertebr. Palaeontol.* 31:727.

Taylor, M. P. (2014). Quantifying the effect of intervertebral cartilage on neutral posture in the necks of sauropod dinosaurs. *PeerJ* 2:e712. doi: 10.7717/peerj.712

Taylor, M. P., and Wedel, M. J. (2013a). The effect of intervertebral cartilage on neutral posture and range of motion in the necks of sauropod dinosaurs. *PLoS One* 8:e78214. doi: 10.1371/journal.pone.0078214

Taylor, M. P., and Wedel, M. J. (2013b). Why sauropods had long necks; and why giraffes have short necks. *PeerJ* 1:e36. doi: 10.7717/peerj.36

Tsuihiji, T. (2005). Homologies of the *transversospinalis* muscles in the anterior presacral region of Sauria (Crown Diapsida). *J. Morphol.* 268, 986–1020. doi: 10.1002/jmor.10294

Tsuihiji, T. (2007). Homologies of the *longissimus*, *iliocostalis*, and hypaxial muscles in the anterior presacral region of extant diapsida. *J. Morphol.* 263, 151–178. doi: 10.1002/jmor.10565

Tykoski, R. S., and Rowe, T. (2004). "Ceratosauria," in *The Dinosauria*, 2nd Edn, eds D. B. Weishampel, P. Dodson, and H. Osmólska (Berkeley, CA: University of California Press), 47–70.

Upchurch, P., Barrett, P., and Dodson, P. (2004). "Sauropoda," in *The Dinosauria*, 2nd Edn, eds D. B. Weishampel, P. Dodson, and H. Osmólska (Berkeley, CA: University of California Press), 259–324.

Vanden Berge, J. C., and Zweers, G. A. (1993). "Myologia," in *Handbook of Avian Anatomy: Nomina Anatomica Avium*, eds J. J. Baumel, A. S. King, J. E. Breazile, H. E. Evans, and J. C. Vanden Berge (Cambridge, MA: Nuttal Ornithological Club), 189–247.

Vidal, D., and Díez Díaz, V. (2017). Reconstructing hypothetical sauropod tails by means of 3D digitization: *Lirainosaurus astibiae* as case study. *J. Iber. Geol.* 43, 293–305.

Vidal, D., Mocho, P., Páramo, A., Sanz, J. L., and Ortega, F. (2020a). Ontogenetic similarities between giraffe and sauropod neck osteological mobility. *PLoS One* 15:e0227537. doi: 10.1371/journal.pone.0227537

Vidal, L. S., Gomes da Costa Pereira, P. V. L., Tavares, S., Brusatte, S. L., Paglarelli, L., and dos Anjos Candeiro, C. R. (2020b). Investigating the enigmatic Aeolosaurini clade: the caudal biomechanics of *Aeolosaurus maximus* (Aeolosaurini/Sauropoda) using the neutral pose method and the first case of protonic tail condition in Sauropoda. *His. Biol.* 1–21. doi: 10.1080/08912963.2020.1745791

Webb, G. J. W., and Gans, C. (1972). Galloping in *Crocodylus johnstoni* – a reflection of terrestrial activity? *Rec. Aust. Mus.* 34, 607–618.

Wedel, M. J. (2003a). The evolution of vertebral pneumaticity in sauropod dinosaurs. *J. Vertebr. Paleontol.* 23, 344–357.

Wedel, M. J. (2003b). Vertebral pneumaticity, air sacs, and the physiology of sauropod dinosaurs. *Paleobiology* 29, 243–255.

Wedel, M. J. (2005). "Postcranial skeletal pneumaticity in sauropods and its implications for mass estimates," in *The Sauropods: Evolution and Paleobiology*, eds J. A. Wilson and K. Curry-Rogers (Berkeley, CA: University of California Press), 201–228.

Wedel, M. J. (2009). Evidence for Bird-like air sacs in saurischian dinosaurs. *J. Exp. Zool.* 311, 611–628. doi: 10.1002/jez.513

Wedel, M. J., Cifelli, R. I., and Sanders, R. K. (2000). Osteology, paleobiology, and relationships of the sauropod dinosaur *Sauroposeidon*. *Acta Palaeontol. Polon.* 45, 343–388.

Wedel, M. J., and Sanders, K. (2002). Osteological correlated of cervical musculature in Aves and Sauropoda (Dinosauria: Saurischia) with comments on the cervical ribs of *Apatosaurus*. *PaleoBios* 22, 1–6.

Wedel, M. J., and Taylor, M. P. (2013). Caudal pneumaticity and pneumatic hiatuses in the Sauropod Dinosaurs *Giraffatitan* and *Apatosaurus*. *PLoS One* 8:e78213. doi: 10.1371/journal.pone.0078213

Wellnhofer, P. (1993). Prosauropod dinosaurs from the Feuerletten (Middle Norian) of Ellingen near Weissenburg in Bavaria. *Rev. Paléobiol. Spéc. Vol.* 7, 263–271.

Wilhite, R. (2003). *Biomechanical Reconstruction of the Appendicular Skeleton in Three North American Jurassic Sauropods*. Ph.D. dissertation. Louisiana State University, Baton Rouge.

Wilson, J. A. (1999). A nomenclature for vertebral laminae in sauropods and other saurischian dinosaurs. *J. Vertebr. Paleontol.* 19, 639–653. doi: 10.1371/journal.pone.0017114

Witmer, L. M. (1995). "The extant phylogenetic bracket and the importance of reconstructing soft tissues in fossils," in *Functional Morphology in Vertebrate Paleontology*, ed. J. J. Thomason (Cambridge: Cambridge University Press), 19–33.

Witmer, L. M. (1997). The evolution of the antorbital cavity in archosaurs: a study in soft-tissue reconstruction in the fossil record with analysis of the function of pneumaticity. *J. Vertebr. Paleontol. Mem.* 3, 1–73.

Yates, A. M., Wedel, M. J., and Bonnan, M. F. (2012). The early evolution of postcranial skeletal pneumaticity in sauropodomorph dinosaurs. *Acta Palaeontol. Polon.* 57, 85–100. doi: 10.1111/j.1469-185X.2011.00190.x

Zug, G. R. (1974). Crocodilian galloping: an unique gait for reptiles. *Copeia* 2, 550–552.

Zurriaguz, V. I., and Cerda, I. A. (2017). Caudal pneumaticity in derived titanosaurs (Dinosauria: Sauropoda). *Cretac. Res.* 73, 14–24.

Zweers, G. A., Vanden Berge, J. C., and Koppendraier, R. (1987). Avian cranio-cervical systems. Part I: anatomy of the cervical column in the chicken (*Gallus gallus* L.). *Acta Morphol. Neerl. Scand.* 25, 131–155.

Conflict of Interest: HM owns company Palaeo3D. He performed all work on this manuscript in his function as an associate researcher with CeNak Hamburg.

The remaining authors declare that the research was conducted in the absence of any commercial or financial relationships that could be construed as a potential conflict of interest.